



1 Human-induced influence on eggs and larval fish transport in a subtropical estuary

2 **Maria Helena P. António^{a,c,*}, José H. Muelbert^b and Elisa H. L. Fernandes^a**

3 ^aLaboratório de Oceanografia Costeira e Estuarina. Instituto de Oceanografia. Universidade Federal do Rio Grande,
4 Brasil

5 ^bLaboratório de Ecologia do Ictioplâncton, Instituto de Oceanografia. Universidade Federal do Rio Grande, Brasil

6 ^cEscola Superior de Ciências Marinhas e Costeiras. Universidade Eduardo Mondlane, Moçambique

7 *E-mail: mhbeula2@gmail.com

8 Abstract

9 The transport during the early stages of life to the nursery areas is one of the main processes
10 in the maintenance of the marine fish population, and human interventions can interfere with this
11 process. In this work, the TELEMAC-3D model coupled to passive particles was used to understand
12 the effect of the change in the configuration of the Barra Jetties of the Rio Grande regarding the
13 transport of eggs and larvae of the croaker *Micropogonias furnieri* in the Patos Lagoon estuary
14 (PLE). Twelve experiments of 5 days that consisted of periods of high and low discharge combined
15 with winds from the south quadrant (SW, S, and SE) were carried out to test the hypothesis that
16 human interventions in the coastal region alter the transport patterns of fish eggs and larvae. The
17 low flow guaranteed a greater extent of saline intrusion and larvae incursion in the estuary, with the
18 opposite occurring in the scenario of high flow. The SW wind ensured the most efficient recruitment
19 into the estuary, in terms of both entry time and maximum reach in both configurations. However,
20 the recent modernization works of the Barra Jetties have changed the pattern of transport and
21 dispersal of larvae and have reduced the amount and reach of the incursion of croaker eggs and
22 larvae into the estuary compared to their old configuration. With the new configuration of jetties,
23 reductions in the larvae concentration and abundance in the estuary were registered at
24 approximately 25% for SW and S winds, 68.6% for SE wind at high discharge, and 0.5% to 1% for
25 winds at low discharge. The lateral stratification in the access channel to the estuary, an important
26 parameter in the larvae transport and distribution between the jetties and the predominant wind
27 direction, was decisive in defining the initiation time of the stratification. With the old
28 configuration, the lateral stratification was established 1 h, 7 h, and 10 h after starting the simulation
29 with the incidence of SW, S and SE winds, respectively. In the new configuration, the lateral
30 stratification was established at the same time only with the SW wind, but with a reduced salinity
31 gradient. In this configuration, only the beginning of stratification was observed at the estuary
32 mouth with S winds, while the stratification was not established with SE winds. This fact influenced
33 the intrusion of saline water and resulted in a smaller number of larvae between the jetties and
34 consequently their transport into the estuary. With the new configuration, a reduction in the
35 maximum penetration of the larvae within the estuary was observed at 1.6 km for high discharge
36 and 2.3 km for low discharge. Despite limitations inherent to the numerical modeling technique, the
37 results obtained corroborate the hypothesis that human interventions in the coastal region change
38 the patterns of transport of fish eggs and larvae. Furthermore, the findings suggest that
39 modernization works of the jetties have contributed to reducing the transport of dependent estuarine
40 species to the Patos Lagoon estuary. Coupled with the knowledge obtained by other research about
41 this species, this knowledge can support provisioning measures for better management of fishery
42 resources in the region.

43 **Keywords:** *Micropogonias furnieri*, larvae transport, anthropogenic effects, ports, Patos Lagoon,
44 TELEMAC-3D



45 1. INTRODUCTION

46 Coastal and estuarine environments are extremely important for the life cycle of various
47 marine organisms (Muelbert and Weiss, 1991; Able, 2005; Whitfield, 2016), which are the most
48 important aquatic resources in the world (Liu and Chan, 2016). In addition to their ecological
49 wealth and capability of providing high rates of primary production and abundance of food,
50 estuaries also serve as a habitat, nursery and protection against predators in early life stages and
51 facilitate the development of numerous marine species (Liu and Chan, 2016; Teodosio et al., 2016).

52 The planktonic phase of species demands attention as a research topic, as it is a
53 characteristic component of the life cycle of most marine organisms (Tiessen et al., 2013), and in
54 fish, it is marked by the stages of eggs and larvae. Changes in transport during these stages have
55 been suggested as one of the important factors that affect the variability of recruitment in marine
56 fish stocks (Brown et al., 2000; Houde, 2008). The survival of fish larvae depends on the pattern of
57 circulation and transport from the spawning to the nursery area, and local biological and physical
58 events can explain the patterns of growth and survival in the early stage of fish life (Lough et al.,
59 1994; Brown et al., 2000; Hinrichsen, 2009; Endo et al., 2019).

60 Studies to understand the pattern of transport and dispersion of eggs and larvae in estuaries
61 and coastal regions in their passive phase have been of great importance for understanding the
62 reduction in the stock of adults in different regions around the world. Lough et al. (1994) evaluated
63 the influence of advection promoted by the wind in the interannual variability and distribution of
64 cod eggs and larvae in the Georges Bank region. Blanton et al. (1999) reported the use of passive
65 larvae of white shrimp and blue crab megalope to understand the response of the wind transport
66 generation over the shallow estuary channel in the southeastern United States.

67 Brown et al. (2000) investigated the importance of tidal forces in the transport of larvae
68 through the narrow channel under the effect of jetties in the bay of Aransas Pass. Sentchev and
69 Korotenko (2007) evaluated the effect of physical forcing and vertical migration on the transport
70 and dispersion of sole larvae in the region of freshwater influence (ROFI) in the east of the English
71 Channel. Tiessen et al. (2013) determined the importance of passive transport by advection in the
72 dispersion of eggs and larvae of plaice fish in the south of the North Sea and the English Channel.
73 Teodosio et al. (2016) described the biophysical processes involved in the recruitment of fish larvae
74 in the Ria Formosa lagoon estuary. Joyeux (2001) evaluated the influence of wind, tide, and
75 meteorological forces in the retention of fish larvae transported to estuaries by the Beaufort channel
76 in North Carolina.

77 The croaker *Micropogonias furnieri* is one of the most important fishery resources in Brazil,
78 with approximately 43.369 tons of catch per year (MPA, 2011). Along the coast of Rio Grande do
79 Sul, in the Patos Lagoon estuary, *M. furnieri* is one of the 3 most abundant species of Sciaenidae
80 (Ibagy and Sinque, 1995) and is considered one of the species with the greatest commercial value in
81 the region (Haimovici and Cardoso, 2017). The species is in decline in the Patos Lagoon region and
82 its catch was reduced from 22,500 tons between 1970-1974 to 7,000 tons captured between 2007-
83 2010 (Haimovici and Cardoso, 2017). Croaker spawns preferentially along the internal continental
84 shelf, near estuarine mouth systems, and can spawn an average of 3 to 7 million eggs over a
85 breeding season (Acha et al., 2008; Albuquerque, 2008; Albuquerque et al., 2009; Bruno and
86 Muelbert, 2009; Acha et al., 2012). It is present throughout the year, and the summer (November to
87 April) is the period of its greatest spawning, consequently of eggs and larvae abundance (Muelbert
88 and Weiss, 1991; Ibagy and Sinque, 1995). In the South Atlantic, the physical mechanisms that
89 determine the success of the transport and recruitment of the early stages of the life of the croaker
90 are consensual and attributed to winds and low river discharge (Muelbert and Weiss, 1991; Ibagy
91 and Sinque, 1995; Acha et al., 1999; Martins et al., 2007; Acha et al., 2012; Costa et al., 2014;
92 Franzen et al., 2019).

93 The Patos Lagoon estuary is known to have favorable conditions for feeding and
94 development for numerous species, both fish and crustaceans (D'Incao, 1991; Salvador and



95 Muelbert, 2019). In this estuary, the dynamics of input and output of estuarine-dependent organisms
96 are controlled by winds and discharges because these are the dominant forces in circulation (Moller
97 et al. 2001; 2009). The recruitment of eggs and larvae in the Patos Lagoon estuary occurs during the
98 spring and summer (Ibágy and Sinque, 1995; Martins et al., 2007; Vaz et al. 2007; Bruno and
99 Muelbert, 2009; Franzen et al., 2019), and the mechanism responsible for its entry into the estuary
100 is the sea level rise on the coast that is generated by the Ekman transport resulting from the south
101 quadrant winds (Vaz et al. 2007). Vaz et al. (2007) highlight that the residual baroclinic current
102 resulting from the contribution of the continental discharge promotes the retention and
103 accumulation of the ichthyoplankton inside the estuary. The dynamics of transport and dispersion of
104 eggs and larvae of the *Micropogonias furnieri* in the Patos Lagoon estuary are determined by
105 weather conditions, such as the direction, intensity and duration of the southwest winds, combined
106 with low discharges, passing each stage of their development in different environments of the
107 estuary (Martins et al., 2007; Bruno and Muelbert, 2009; Franzen et al., 2019).

108 Changes in the topography and natural geomorphological structure of the access channels
109 impact the dynamics and ecology of estuaries (Yuk and Aoki, 2007; Liu and Chan, 2016).
110 Specifically, concerning the transport of fish eggs and larvae, studies show that there is a direct
111 correlation between recruitment and environmental conditions during their transport, making
112 anthropogenic contribution one of the processes that limit stock and recruitment (Hinrichsen, 2009;
113 Acha et al., 2012). In 2010, modernization works were completed at the mouth of the Patos Lagoon
114 estuary (Moller and Fernandes, 2010). The Barra Jetties, built-in 1915, had an increase in the length
115 of approximately 10% and 18% (370 m and 700 m) on the east and west side, respectively, as well
116 as a reduction of approximately 15% in the opening width (currently with 700 m). An increase in
117 the depth in the navigation channel was followed by a reduction in saline intrusion and the current
118 speed that was associated with the modifications made (Lisboa and Fernandes, 2015; Silva et al.,
119 2015). Recently, António et al (submitted) found that changes in the access channel and Barra
120 Jetties caused a reduction in saline intrusion, a reduction of approximately 20% in both flooding and
121 ebbing speeds, and a reduction in the time of occurrence of lateral stratification events between the
122 jetties by approximately 1/3 from the old to the new jetty configuration. These changes in the
123 characteristics of estuarine circulation may have an impact on the transport and dispersion of eggs
124 and fish larvae in the PLE.

125 The high cost and the difficulty in obtaining data in situ with adequate space-time resolution
126 for analyzing the complexity of coastal ecosystems have limited its studies. The numerical
127 modeling technique, coupling hydrodynamic and biological models, has been increasingly used as a
128 tool to solve this limitation (Lough et al., 1994; Brown et al. 2000; Seiler et al., 2015; Franzen et al.,
129 2019). The physical-biological coupling has ensured better coverage by interpolation and
130 extrapolation of data in the space-time domain, assisting in fish dynamics studies at an early stage
131 of life. These advances have enabled us to understand the causes of mortality of larval and juvenile
132 fish during transport, focusing on the effects of advective and tropodynamic processes (Brown et
133 al. 2000; George et al, 2011; Seiler et al., 2015). Lagrangian models of particle transport consider
134 eggs and larvae to be passive particles, allowing the monitoring of their trajectory from the
135 spawning site to their final deposition (Blanton et al., 1999; Brown et al. 2000; Martins et al., 2007;
136 Vaz et al. 2007; Acha et al., 2012).

137 The main objective of the present study is to determine if the modification of the Barra
138 Jetties of the Rio Grande influences the transport of eggs and larvae of the croaker, *Micropogonias*
139 *furnieri*, in the Patos Lagoon estuary. For this, the hydrodynamic model TELEMAC-3D with
140 passive particles will be used. The results of this study aim to contribute to an understanding of the
141 new dynamics of the recruitment process and management of fishery resources of the Patos Lagoon
142 and the adjacent coastal region.

143 1.1. Study Area



144 The Patos Lagoon (Figure 1) is located in the southwestern region of Brazil between 30° and
145 32° South. It is classified as a strangled coastal lagoon (Kjerfve, 1986) that is 250 km long, 40 km
146 wide, and an average depth of 5 m, occupying an area of approximately 10,360 km² (Moller et al.,
147 2001). The lagoon is connected to the South Atlantic Ocean by a narrow channel less than 1 km
148 wide (Martins et al., 2007). The estuarine region of the Patos Lagoon, which represents
149 approximately 10% of the total area of the lagoon, has more than 80% of its area with depths below
150 2 m and has a diversity and abundance of flora and fauna, which makes these local areas suitable
151 for the development of estuarine-dependent organisms (Moller et al., 2001; Odebrech et al., 2010).

152 The lagoon has 3 main tributaries, the Guaíba River, the Camaquã River, and the São
153 Gonçalves Channel, with an average discharge of approximately 2400 m³s⁻¹, ranging between 700
154 m³s⁻¹ during the summer and 3000 m³s⁻¹ during spring (Moller et al., 2001; Moller and Fernandes,
155 2010). Tides have little influence on the estuary dynamic (which is defined by winds and
156 discharges), presenting a diurnal predominance with an amplitude of approximately 0.3 m and is
157 attenuated during the propagation toward the estuary (Moller et al., 2001; Fernandes et al., 2004;
158 Moller et al., 2009). Its greatest contribution is in modulating the mixture of the water column and
159 transporting water further to the north of the estuary during periods of less intense winds and
160 discharges (Moller and Fernandes, 2010).

161 The winds and discharge regime delimit the range of saline intrusion in the Patos Lagoon,
162 and in low discharges, the salinity can pass the northern limit of the estuarine region (Moller et al.,
163 2001; Moller and Fernandes, 2010; Seiler et al., 2015). In contrast, the high discharges function as
164 physical barriers, not allowing the intrusion of saltwater into the estuary, which may affect the
165 pattern of recruitment, immigration, and emigration of organisms of estuarine species (Garcia et al.,
166 2001; Salvador and Muelbert, 2019).

167 2. METHODOLOGY

168 The present study was based on the application of the hydrodynamic numerical model
169 TELEMAC-3D (www.opentelemac.org) and its Lagrangian module to investigate the influence of
170 configuration change of the Barra Jetties of the Rio Grande on the transport and dispersion of eggs
171 and larvae of the croaker, *Micropogonias furnieri*, in the Patos Lagoon estuary. Controlled
172 simulations were carried out, considering extreme discharge conditions and winds from the south
173 quadrant.

174 2.1. Hydrodynamic Numerical Model

175 The TELEMAC-MASCARET model (V7P0 version) was developed by *Laboratoire*
176 *National d'Hydraulique et Environnement of the Company Electricité of France (©EDF)*. The
177 model presents modules in two and three dimensions to study hydrodynamics, sediment transport,
178 waves, and water quality of coastal regions. The hydrodynamic model solves the Navier-Stokes
179 Equations, considering local variations of the free surface of the fluid, neglecting the variation of
180 density in the mass conservation equation, considering the hydrostatic or non-hydrostatic pressure
181 and the Boussinesq approximation to solve the equation of motion. The model applies the Finite
182 Element Method in order to solve the hydrodynamic equations, using the Sigma Coordinate System
183 for vertical discretization. The model domain is discretized by a non-structured grid of finite
184 elements (triangular elements), which allows concentrating a higher number of elements in regions
185 of interest and/or significant bathymetric variations, and lower resolution in regions of more
186 homogeneous bathymetry, reducing computational time. Details about the model formulations are
187 presented by Hervouet (2007).

188 The bathymetry of the Patos Lagoon, the estuary, and the adjacent coastal region was
189 obtained from historical data. Nautical charts from the Directory of Hydrography and Navigation
190 (DHN, Brazilian Navy) before 2010 were used as the "old" bathymetric information (before
191 changes in configuration). Data from the jetty expansion project were used to define the bathymetry



192 after the alteration of the jetties. The main difference between the two grids is the length of the
193 jetties and the depth of the access channel to the estuary (Figure 1D and 1E). The BlueKenue
194 Software was used to generate the unstructured bathymetric grids of triangular elements. Grid
195 optimization was made in the complex morphology and shallow areas inside the estuary and at the
196 adjacent coastal region, allowing higher resolution in regions of interest. Two resulting meshes were
197 used to reproduce the hydrodynamics before and after the modification of the jetties (Figures 1D
198 and 1E). The meshes encompass the entire study area up to about 2500 m depth to better represent
199 the coastal dynamics.

200 The open boundaries of the domain were forced with results from regional and global
201 models and field data. To be comparable, simulations for both scenarios had the same set-up. Time
202 series of daily averaged river discharge of the main tributaries (Guaíba river and Camaquã river,
203 Figure 1) were obtained from the National Water Agency (www.ana.gov.br) and prescribed at the
204 northern and central continental boundaries. The mean discharge data for the São Gonçalo Channel
205 was considered constant as 700 m³/s (Vaz et al., 2006), as there were no time series of discharge for
206 the studied periods. Temperature and salinity fields obtained from the HYCOM model (Hybrid
207 Model Coordinate Oceanic, <https://hycom.org/>), with a temporal resolution of 3h and spatial
208 resolution of 1/12.5°, were prescribed tridimensionally in all grid points. Wind time series, with a
209 spatial and temporal resolution of 0.75° and 6h, respectively, were obtained from the ECMWF
210 (European Center for Medium-Range Weather Forecasts, www.ecmwf.int). Eleven (11) sigma
211 levels were considered in the vertical and distributed from the bottom to the sea surface.

212 The model calibration and validation for both scenarios (Supplement A) are presented in
213 more detail by António et al. (2020, submitted). The calculated results were compared with field
214 data for the period between October and November 2006 for the old jetty configuration and October
215 to November 2010 for the new configuration. The model performances (Table 1, Supplement A)
216 ranged from Good to Excellent considering the Root Mean Square Error (RMSE) and the Relative
217 Mean Absolute Error (RMAE) results (Wastra et al., 2001). Current velocity time series were used
218 for calibration tests (Figure A1, Supplement A) and salinity, sea surface elevation and current
219 velocity time series were used for validation tests (Figure A2 and A3, Supplement A) for both
220 configurations.

221 2.2. Particle Tracking Model

222 The particle model is a subroutine of the hydrodynamic model TELEMAC-3D, which is
223 simulated internally at each time step after the hydrodynamic component. Therefore, to reproduce
224 the transport of eggs and larvae in the passive phase and simulate their dispersion in the Patos
225 Lagoon estuary, the Lagrangian model was coupled to the hydrodynamic model TELEMAC-3D.

226 The particle model obtains the Lagrangian information from the Eulerian velocity
227 information that is calculated by the hydrodynamic model to determine the particle trajectory
228 caused by the flow at each time step, and the three-dimensional trajectories are computed using the
229 position information calculated at each step of the time.

230 The horizontal and vertical advection movement considers that the Euler scheme and the
231 particle buoyancy are based on the zonal, meridional and vertical components (u, v and w) and is
232 given by the following expressions:

$$X_i(x_0, y_0, z_0)^{n+1} = X_i(x_0, y_0, z_0)^n + \int_{t_0+n\Delta t}^{t_0+(n+1)\Delta t} u_i(x_0, y_0, z_0, t) dt$$

233 where X_i is the position, for horizontal (x_0, y_0) and vertical (z_0) position of the particle movement; u_i is
234 the velocity for a zonal (x_0), meridional (y_0) and vertical (z_0), u, v and w velocity component, respectively; t
235 is the time and Δt is the time step.

236 The calculation of hydrodynamic components is taken into account in a discrete three-
237 dimensional way at each point of the numerical grid. During the simulation, the particles are free to



238 move to any position between the grid points. In each new time step, the velocity is interpolated
239 instantly for each position where the particles are located. The accuracy and resolution of particle
240 transport calculations are extremely dependent on hydrodynamic terms.

241 In this study, a time step of 60 s was applied, with the particle model in phase with the time
242 step of the hydrodynamic model. Thus, at every 60 seconds, TELEMAC-3D runs the hydrodynamic
243 component, and the results are instantly inserted into the particle model, with the displacement of
244 the particles being calculated three-dimensionally in the numerical grid.

245 2.3. Model Experiments

246 To investigate the effect of the modifications made in the Barra Jetties of the Rio Grande on
247 the transport and dispersion of eggs and larvae of *Micropogonias furnieri* in the Patos Lagoon
248 estuary, a total of 12 controlled experiments were carried out, with dynamic forces from extreme
249 conditions of continental discharge combined with constant south quadrant winds (SW, S, and SE),
250 considering the old and the new configuration of the Barra Jetties (Table 1).

251 Table 1: Controlled experiments simulations

Wind direction	Low discharge (La Niña, 2012)		High discharge (El Niño, 2003)	
	Old configuration	New configuration	Old configuration	New configuration
SW	X	X	X	X
S	X	X	X	X
SE	X	X	X	X

252 The simulations were carried out for the first 5 days of January, which represented the
253 passage of cold fronts and ensured the continuous incidence of winds from the south quadrant in the
254 region. Extreme high and low discharge regimes for the years 2003 and 2012, respectively, were
255 considered. These extreme discharge regimes are associated with ENSO, with high discharge
256 characteristics during El Niño (2003) and low discharges during La Niña (2012) (Moller and
257 Fernandes, 2010). Constant SW, S, and SE winds were also considered with an initial intensity of 8
258 m.s⁻¹, decreasing linearly after the second day of incidence until reaching 4 m.s⁻¹ on day 5. South
259 quadrant winds were considered to be those that facilitate the entry of saltwater into the estuary
260 (Moller et al, 2001).

261 The simulation time of 5 days considered the growth rate of the larvae of the species under
262 study and their passive period in the plankton. Eggs of the *Micropogonias furnieri* hatch in up to
263 approximately 24 hours (Albuquerque, 2008), and the larvae are approximately 1.85 mm. The
264 average growth rate is 0.36 mm/day (Albuquerque et al., 2009), and at the end of 5 days after
265 spawning, the larvae will be approximately 3.29 mm. The spawning of the particles was done only
266 once, at the mouth of the Patos Lagoon estuary (Figure 1D and 1E), considering the grouped
267 spawning characteristic of the species. The spawning site was defined based on past studies by
268 Martins et al. (2007) and Franzen et al. (2019), who concluded that the spawning at the estuary
269 mouth guarantees the best recruitment of eggs and larvae of the croaker to the Patos Lagoon
270 estuary.

271 Due to the computational limitation of the TELEMAC-3D version V7P0, the maximum
272 particle concentration per defined spawning area was 7000 for each simulation. This number of
273 particles represents approximately 25% of the maximum average concentration of eggs per cubic
274 meter (497 eggs/100 m³) (Bruno and Muelbert, 2009). Then, for each experiment run, 7000 particles
275 were placed at a depth of 5 m at 00:00 on January 1, 2003 (high discharge) and January 1, 2012
276 (low discharge). The evolution of the larvae was monitored for 5 days.



277 Eggs and larvae were considered passive and neutral particles, assuming that fish eggs are
278 transported by the flow without depositing. During the simulation, the particles were considered
279 eggs from the spawning site for up to 24 hours, and shortly afterward, the occurrence of hatching of
280 the eggs was considered when the particles started to be considered larvae of the *Micropogonias*
281 *furnieri* croaker. The abundance of eggs and larvae in a given region is affected by predators, by the
282 rate of growth and mortality, but these processes were not considered in the present study due to the
283 limitations of the Lagrangian model.

284 2.4. Data Processing

285 Numerical simulations that considered the old and the new configuration of the Barra Jetties
286 of the Rio Grande and the incidence of constant winds of the south quadrant (Figures 2A - 2F) in
287 periods of high (Figure 2G) and low (Figure 2H) continental discharge were analyzed
288 comparatively for the 6 simulated scenarios (Table 1).

289 The results were analyzed in relation to the extension of entry of larvae and eggs and their
290 distribution in the estuary. Maps of spatial patterns of the salinity field and the final distribution of
291 the larvae in the estuary in the last step of the simulations for the periods of high and low discharge
292 during the incidence of southern winds were selected for presentation.

293 Based on the sampling techniques proposed by Cochran (1976) and based on simple
294 significant sampling calculations made by Miaoulis and Michener (1976), stratified random samples
295 of 99 larvae, which represented a 10% precision level (sampling error), a 95% confidence level and
296 a variability degree (proportion) $P = 0.5$, were extracted from the total of 7000 placed in the
297 simulations (Cochran, 1976; Miaoulis and Michener, 1976; Israel, 1992). To determine the average
298 path taken by the larvae at the end of each day in the two configurations (old and new), the
299 weighted distances traveled by each of the larvae that compose the sample were calculated from the
300 spawning place (in the mouth of the estuary) until the end of each of the 5 days of simulation. Then,
301 the center of mass was found, calculating the average distance covered at the end of each day.
302 Finally, the mean standard deviation of the individual distances from the center of mass (mean
303 distance) was calculated. The Student's t-test was applied to verify the significance between the
304 average distances in the two configurations in the simulated scenarios (Louangrath, 2015;
305 Padovani, 2012). At random, another reduced sample of 10 larvae (P1, P2, P3, P4, P5, P6, P7, P8,
306 P9, and P10) was extracted at the end of each day, and the trajectories of larvae were tracked from
307 the spawning site to the final location in the two configurations (old and new) of the Barra Jetties, at
308 the end of each of the five simulation days.

309 The abundance of larvae for each hydrodynamic simulation was extracted from the model
310 result for 6 areas (A1, A2, A3, A4, A5 and A6 (Figure 1C)) at the end of each of the five simulation
311 days and analyzed in terms of the distribution of the spatiotemporal concentration along the estuary.

312 To investigate changes promoted by lateral stratification in the distribution of eggs and
313 larvae between the Barra Jetties, profiles of the spatial distribution of salinity and eggs and larvae
314 were extracted between the Barra Jetties during the flood period. Changes in the time of occurrence
315 of lateral stratification and the salinity gradient were observed in the hydrodynamic study with
316 dynamic winds (António et al., 2020, submitted). In this way, the aim is to evaluate the effect of the
317 difference in the direction of the incident wind (SW, S, and SE) on the variability of the behavior of
318 the lateral stratification, and consequently on the changes in the distribution of eggs and larvae that
319 occurred due to the recent modernization works.

320 To associate the direction of the incident wind and the position (west, center channel and
321 east) of the eggs and larvae among the jetties, the internal area between the west and east Jetties was
322 divided into 3 (three) regions: root, center and mouth of the jetties (mouth). Each of these areas was
323 subdivided into 3 other areas (west, center channel and east jetties), totaling 9 areas, where the
324 concentrations of eggs and larvae were counted during the occurrence of lateral stratification and
325 incidence of SW, S and SE winds.



326 3. RESULTS

327 The periods of extreme discharges used in the experiments (Figure 2) presented different
328 characteristics. During the high discharge period (El Niño, January 2003), the average discharge
329 was $6340 \text{ m}^3\text{s}^{-1}$, the maximum was $8000 \text{ m}^3\text{s}^{-1}$ (on January 2), and the minimum was $5000 \text{ m}^3\text{s}^{-1}$ (on
330 January 5). In contrast, in the low discharge period (La Niña, January 2012), it was practically
331 constant at $1200 \text{ m}^3\text{s}^{-1}$ over the 5 days.

332 3.1. Saltwater Distribution

333 During the period of high continental discharge, the penetration of saltwater was relatively
334 less in the new configuration in the 3 simulated wind scenarios (Figure 3). During SW winds, the
335 salinity in the new configuration (Figure 3D) reached 54 km, approximately 3 km less than the old
336 configuration, which reached 57 km (Figure 3A). During the S wind, salinity reached 43 km in the
337 old configuration (Figure 3B) and 41 km in the new configuration (Figure 6E). During the SE wind,
338 the salinity reached 36 km and 34 km in the old (Figure 3C) and the new (Figure 3F) configuration,
339 respectively.

340 In the low discharge period, the extent of saltwater intrusion passed from the northern limit
341 of the Patos Lagoon estuary in all simulations (Figure 4). The results indicate that the lagoon was
342 less saline in the new configuration in relation to the old configuration during the SW wind, and
343 during the S and SE wind, the saltwater intrusions did not present any noticeable differences. At the
344 end of the 5 days of simulation, the 5 psu isohaline reached approximately 106 km in length in the
345 old configuration (Figure 4A) during the incidence of the SW wind. In the new configuration, the
346 saline intrusion was reduced to 97 km (Figure 4D). During the S wind, the saline intrusion had an
347 extension of approximately 96 km both in the old (Figure 4B) and in the new configuration (Figure
348 4E). The SE wind was the one that presented the least saline intrusion. The salinity for the old
349 (Figure 4C) and new (Figure 4F) configuration reached approximately 79 km.

350 3.2. Transport and Dispersion of Larvae

351 A reduction in the extent of larval transport after the modernization works was observed in
352 the 3 simulated wind scenarios for the period of high (Figure 5) and low continental discharge
353 (Figure 6). The SW winds were the ones that guaranteed the largest incursion of the larvae in the
354 high and low discharge, both for the old configuration (Figures 5A and 6A) and the new
355 configuration (Figures 5D and 6D).

356 At high discharge, during the SW wind, the larvae extension was approximately 58 km and
357 56 km for the old and new configuration, respectively (Figure 5A and 5D). The S and SE winds did
358 not show great differences in their extension between the old and the new configuration. The length
359 varied between 42 km and 40 km for the S wind (Figure 5B and 5E) and between 38 km and 37 km
360 for the SE wind (Figure 5C and 5F) for the old and new configuration, respectively. Differences in
361 the final location of the larvae were observed that were associated with the direction of the incident
362 wind because, during the SW and S wind, the larvae were closer to the east side of the lagoon, while
363 the opposite was observed during the SE wind incidence.

364 Differences in the extension of larvae penetration were noticeable mainly in low discharge,
365 with their pattern associated with the variability of the direction and intensity of the incident wind
366 (Figure 6). The highest concentrations were observed along the navigation channel, with few larvae
367 entering the shallow region of the bags (Arraial and Mangueira, Figure 1). The larvae showed a
368 greater extension than that defined by the 5-psu salinity isohaline into the estuary in both
369 configurations, with greater emphasis on low discharge. At low discharge, the maximum larvae
370 penetration was approximately 109 km from the spawning site to the old (Figure 6A) and
371 approximately 104 km to the new (Figure 6D) configuration of the Barra Jetties. During the
372 incidence of the S wind, the larvae were transported up to approximately 102 km in the old



373 configuration (Figure 6B), and in the new configuration (Figure 6E) up to approximately 101 km.
374 On the other hand, during SE winds, the larvae were transported up to less than 79 km, reaching
375 approximately 78 km in both configurations (old and new, Figure 6C and 6F, respectively). During
376 the incidence of SW winds, the larvae were transported along the central region of the lagoon with
377 different dispersion patterns. In contrast, during the incidence of the S wind, the larvae were
378 transported along the west side of the lagoon in the new configuration (Figure 6E) and through the
379 central cell of the lagoon in the old configuration (Figure 6B). Similarly, during SE winds, the
380 larvae were transported closer to the west side of the lagoon (Figure 6C and 6F) with little
381 dispersion.

382 The total number of larvae transported to the interior of the estuary differed from the old to
383 the new configuration in each incident south wind (Table 2). At high discharge, the transport was
384 greater in the old configuration, with more than 6000 (approximately 87%) larvae inside the estuary
385 in each incident wind (SW, S, and SE). On the other hand, in the new configuration, there was a
386 reduction in the number of larvae transported according to the incident winds. SW and S winds
387 carried slightly more than 4000 (~ 61.5%) larvae, differing by approximately 25.5% from the old
388 configuration, while the SE wind carried only 1287 (~ 18.4%) larvae, a difference of approximately
389 68.6% from the old configuration. In contrast to the high discharge, in the low continental
390 discharge, the difference in the transport of larvae to the lagoon between the old and the new
391 configuration of the jetties fluctuated between 0.5% and 1% according to the winds. SW and SE
392 winds were the ones that transported the most larvae to the interior of the estuary in both
393 configurations (old and new), with more than 6000 (~ 86%) larvae each. The S wind carried just
394 over 5000 (~ 72%) larvae in both configurations.

395 Table 2: Total number and percentage of larvae of *Micropogonias furnieri* transported towards the
396 estuary at the end of the 5 days of simulation, during south quadrant winds for the old and new
397 configurations.

Wind Direction	Configuration	High Discharge	Low Discharge
SW	Old	6100 (87%)	6000 (85%)
S	Old	6016 (86,9%)	5101 (72,9%)
SE	Old	6101 (87,2%)	6200 (88,6%)
SW	New	4400 (62,9%)	6003 (85,8%)
S	New	4210 (60,1%)	5003 (71,5%)
SE	New	1287 (18,4%)	6102 (87,2%)

398 In the adjacent coastal region, it was observed that some larvae that did not enter the estuary
399 were transported to the north during SW winds (Figure 5A and 5D, 6A, and 6D), leaving the range
400 of the area of interest in both configurations. During the S winds (Figure 5B and 5E, 6B and 6E), a
401 portion of the larvae was trapped at the mouth of the estuary in the coastal region adjacent to the
402 east of the Barra Jetties. During the incidence of SE winds (Figure 5C and 5F, 6C and 6F), the
403 larvae were also concentrated in the coastal region adjacent to the mouth of the estuary. In contrast
404 to the high discharge, in the low discharge, the old and the new configuration did not present
405 notable differences in the dispersion of the larvae in the coastal region. However, as in the high
406 discharge, at low discharge, larvae that did not enter the estuary showed a similar dispersion pattern.

407 3.3. Larvae Travel Distance



408 Figure 7 shows the evolution of the average distance traveled by the particles at the end of
409 each simulation day for the high (Figure 7A) and low (Figure 7B) discharge period during SW
410 winds. This wind condition was chosen because it guaranteed the largest incursion of larvae into the
411 estuary in comparison to the S and SE winds (Figures 5 and 6).

412 During the high discharge period, at the end of the first day, the eggs covered an average of
413 13 km in the old and 9.5 km in the new configuration of the Barra Jetties (Figure 7A). On the
414 second day, the distance covered reached approximately 22.5 km and 19 km in the old and the new
415 configuration, respectively. On the third day, they passed the central region of the estuary, reaching
416 35 km and 30.5 km. On the fourth day, the distance covered was reduced; in the old configuration,
417 the larvae reached approximately 39.5 km, and in the new configuration, they reached
418 approximately 35.5 km. This trend was maintained, with the fifth day being the shortest route for
419 the larvae, reaching an average distance of 45 km and 43 km in the old and the new configuration,
420 respectively. These differences in the mean distance were not statistically significant ($p = 0.6857$).

421 At low discharge (Figure 7B), the particles passed the northern limit of the estuary (Ponta de
422 Feitoria, Figure 1A). On the first day, the particles traveled approximately 17.5 km in the old
423 configuration and approximately 13.5 km in the new configuration. On the second day, they reached
424 approximately 31 km and 26 km away, in the central region of the estuary, in the old and new
425 configuration, respectively. On the third day, they reached approximately 49.5 km and 45 km. On
426 the fourth day, different from what was observed in the high discharge, the distance covered
427 increased in both configurations (old and new), and the larvae reached approximately 65.5 km and
428 60.5 km. This trend was maintained, and on the fifth day, the larvae reached an average distance of
429 94 km and 89 km in the old and new configurations, respectively. Similar to the high discharge, at
430 low discharge, the differences in the average distance between the old and the new configuration
431 were not statistically significant ($p = 0.8099$).

432 At the end of each day, the larvae traveled long distances in the old configuration of the
433 Barra Jetties, at both high and low discharge. At high discharge (Figure 7A), the distances traveled
434 by the larvae in the two configurations decreased from day 1 to day 5. The difference on the first
435 day was approximately 3.5 km, gradually reducing to approximately 2 km on the fifth day. The
436 average distance traveled at the end of each day was similar for both configurations, ranging from
437 approximately 9.5 km from the first to the second day, increasing by approximately 12.5 km from
438 the second to the third, and then decreasing to 4.5 km and 5.5 km in the old and new configuration,
439 respectively. At low discharge (Figure 7B), the average travel difference between the two
440 configurations was approximately 4 km on the first and second days. On the third day, the
441 difference between the two configurations increased to 4.5 km, while reducing on the fourth day to
442 4 km. On the fifth day, the difference was fixed at 5 km.

443 3.4. Larvae Trajectories

444 To study the evolution of the particle trajectory over time, the transport behavior of 10 larvae
445 was analyzed from the first hour (1 hour) to the end of 5 days of simulation for both configurations
446 of the Barra Jetties, during the high and low period (Figure 8) discharge. Experiments with an
447 incidence of the SW wind were analyzed because they ensured the largest incursion of larvae into
448 the interior of the Patos Lagoon compared to the S and SE winds.

449 The largest length of the trajectory traveled by the larvae was observed in the old
450 configuration both at high (Figure 8A and 8B) and low (Figure 8C and 8D) discharge. During the
451 period of high continental discharge, most of the tracked larvae entered the estuary in the old
452 (Figure 8A) configuration compared to the new (Figure 8B) configuration of the Barra Jetties. The
453 other larvae stayed in the adjacent coastal region (Figures 8A and 8B) and moved to the north. The
454 greater extension in the daily trajectory traveled by the same larva at the end of each day led the
455 larvae to position themselves in distant locations between the two configurations, a fact that was
456 reflected in the final position. Of the larvae that entered the estuary, it was also observed that in the



old configuration of the jetties (Figure 8A), some larvae had their trajectory in the bags of Mangueira and Arraial (Figure 1A), while in the new configuration of the jetties (Figure 8B), none of the larvae entered into the bags. At low discharge, the tracked larvae behaved similarly to the high discharge. The larvae that entered the estuary differed in length by covering greater distances in the old configuration, and it was also observed that larvae entered into the bags only in the old configuration of the jetties (Figure 8C).

3.5. Spatiotemporal Distribution of Eggs and Larvae

Figure 9 shows the spatiotemporal evolution of eggs and larvae concentration in 6 areas of the Patos Lagoon estuary (Figure 1C) over the 5 days of simulation during the period of high continental discharge. For all tested wind scenarios (SW, S, and SE), the number of larvae that reached regions A1, A2, A3, A4, A5, and A6 differ from each other when comparing results for the old and the new configuration of the jetties.

During the beginning of the simulation of the high discharge, the two days preceding the simulations (day 30 and 12/31/2002) presented winds from the south quadrant (Figure 2A, 2C, 2D), driving the early entry of the plume into the interior of the estuary. One hour after the start of the simulation, area A1 showed approximately 100% (~ 7000) of eggs in the old configuration and approximately 61% (~ 4300) of eggs in the new configuration, and no eggs were recorded in the remaining estuary areas during SW winds (Figure 9A); a similar situation was verified during S and SE winds (Figure 9G and 9M). At low discharge, one hour after the simulation started, area A1 showed only a concentration of approximately 36% (~ 2500 of 7000) of eggs in the old configuration, while in the new one, there were no eggs in the estuary for any of the incident winds. (Figure 10A, 10G and 10M).

On day 1, during the SW wind (Figure 9B), the larvae reached area A3, concentrating the largest number of larvae in area A2 in both the old and the new configuration. However, different from the old configuration that already concentrated more than 75% of the larvae, in the new configuration, the total of the larvae in areas A1, A2 and A3 represented less than 50%. During the S wind (Figure 9H), in both configurations, the larvae reached area A2 where they concentrated their greatest abundance of approximately 94% and 84% for the old and new configuration, respectively. On the other hand, during the SE wind (Figure 9N) at the end of the day1, in the old configuration, the larvae reached area A2, and almost 100% of the larvae concentrated in these 2 areas. However, in the new configuration, the larvae were restricted to area A1 with only approximately 26% of the larvae.

On day 2, during the SW wind (Figure 9C), the larvae reached area A4, with the greatest abundance in area A3 in both configurations; an abundance of approximately 85% in the old configuration was shown, while that in the new configuration was approximately 64%. During the S wind (Figure 9I), the larvae reached area A3, registering the greatest abundance in this area, but a reduction in the total number of larvae in the areas within the estuary was observed compared to day 1. The old configuration presented approximately 71%, and the new configuration presented only approximately 15% of the larvae. During the SE wind (Figure 9O), the distribution of the larvae did not pass from area A2 in both configurations, and similar to the S wind, a reduction in the total number of larvae inside the estuary was observed, reducing to approximately 54% in the old configuration and approximately 20% for the new configuration.

On day 3, concentrations increase again in the 3 winds studied (Figures 9D, 9J, 9P). During the SW wind (Figure 9D), the larvae reached area A5 (northern limit of the estuary, Figure 1C), with a greater abundance in area A4 in both configurations. A total of approximately 87% (~ 6,100) of the larvae were recorded in the old configuration and approximately 60% (~ 4,200) in the new configuration. During the S wind (Figure 9J), the larvae reached area A4 in both configurations, and the abundance in the old configuration was approximately 86% (~ 6050), and in the new configuration, the total larvae did not exceed 15% (~ 1030). During the SE wind (Figure 9P), the



506 larvae reached area A4 in the old configuration where the greatest abundance occurred, while in the
507 new configuration, area A3 was restricted, and the greatest abundance was observed in area A1. The
508 total number of larvae was approximately 86% (~ 6060) in the old configuration and approximately
509 61% (~ 4300) in the new configuration.

510 On day 4, during the SW wind (Figure 9E), the larvae did not pass area A5, showing only an
511 increase in abundance in area A5, and the total larvae did not change in both configurations. During
512 the S wind (Figure 9K), the larvae reached area A5 despite the greater abundance being
513 concentrated in area A4, as observed on day 3 in both configurations. The total number of larvae
514 inside the estuary did not change in the old configuration, remaining at approximately 86% (~
515 6050), while the new configuration registered an increase of approximately 62% (~ 4400). During
516 the SE wind (Figure 9Q), the larvae did not pass area A4 in both configurations, concentrating
517 approximately the total of the larvae in this area in the old configuration with an abundance of
518 approximately 86% (~ 6060). In contrast, in the new configuration, the larvae were distributed in all
519 areas with a total abundance of approximately 18% (~ 1260).

520 On the last day of the simulation (day 5), the total number of larvae did not change from day
521 4 in both configurations for the 3 winds studied. During the SW wind (Figure 9F), the larvae passed
522 from the northern limit of the estuary (Figure 1C) and reached area A6 in both configurations, with
523 their greatest abundance in area A5. During the S wind (Figure 9L), the larvae distribution was
524 limited to area A5 in both configurations, concentrating their abundance between areas A4 and A5.
525 During the SE wind (Figure 9R), the old configuration showed a decrease in the larvae incursion,
526 and the greatest abundance was observed in area A3 in the new configuration, where the distribution
527 of abundance was approximately similar in all areas.

528 In the low continental discharge, 1 h after starting the simulations for the 3 winds studied
529 (SW, S, and SE) (Figure 10A, 10G, 10M), only in the old configuration did the larvae enter the
530 estuary, concentrating the larvae in area A1 with an abundance of approximately 36% (~2500).

531 On day 1, during the SW wind (Figure 10B), the larvae in the old configuration passed from
532 the northern limit of the estuary (A5, Figure 1C) and reached area A6 in the old configuration, with
533 a greater abundance in area A4. In contrast, in the new configuration, the larvae did not pass area
534 A3 where the greatest abundance was observed. Unlike the old configuration that had the largest
535 incursion of larvae in the estuary, the new configuration presented the largest number of larvae in
536 approximately 81% (~5700) compared with approximately 71% (~5000) of the old configuration.
537 During the S wind (Figure 10H), the larvae reached area A4 in the old configuration, while in the
538 new configuration, the larvae did not pass area A3 where the greatest abundance was observed in
539 both configurations. The total abundance was approximately 76% (~5300) in the old configuration
540 and approximately 24% (~1700) in the new configuration. During the SE wind (Figure 10N), in the
541 old configuration, the larvae also reached the northern limit of the estuary, area A5, concentrating
542 their greatest abundance in area A4. In contrast, in the new configuration, the larvae did not pass
543 area A3, concentrating the greatest abundance in the areas A1 and A2 on the lower estuary. As
544 observed during the SW wind, in the SE wind, the new configuration presented the highest total
545 abundance of approximately 92% (~6500) compared to approximately 85% (~ 6100) in the old
546 configuration despite the lesser incursion.

547 From day 2 (Figure 10C, 10I, 10O), the larvae in the old configuration passed from the
548 northern limit of the estuary (area A5, Figure 1C) during all winds (SW, S, and SE), spreading
549 toward the north of the Lagoon, whereas in the new configuration, this only occurred during the SW
550 wind. The concentration of larvae declined from region A1 until up to the limit of the estuary (area
551 A5), with total abundance declining to 57% (~4000) and 47% (~3300) for the old and new
552 configuration, respectively, concentrating the largest number of larvae in area A4 (Figure 10C) in
553 both configurations. The S wind showed the same behavior only for the old configuration, where
554 the abundance declined to approximately 74% (~5150), while in the new configuration, the larvae
555 were limited and concentrated their greatest abundance in area A4, and their total abundance



556 registered an increase of approximately 73% (~5100) (Figure 10I). The SE wind showed almost no
557 larvae from area A4 (Figure 10O) in the new configuration, whereas the old configuration showed
558 its greatest abundance in area A6. The new configuration presented its abundance distributed in
559 areas lower than A4 (A1, A2, and A3). Similar to the SW wind, the SE wind showed a decline in
560 total abundance to approximately 71% (~ 5000) in the old and approximately 86% (~6000) in the
561 new configuration.

562 On day 3 (Figure 10D, 10J, 10P), the decay of larvae abundance continued in the region of
563 the estuary (A1 to area A5) for all winds, demonstrating the incursion of the larvae beyond the
564 estuarine region. During the SW wind (Figure 10D), in the old configuration, the abundance
565 dropped to 36% (~2500), and in the new configuration, the larvae reached and passed the northern
566 limit of the estuary, with their total abundance dropping to 60% (~4200). During the wind S (Figure
567 10J), the abundance declined to approximately 69% (~4800) and approximately 31% (~2200) in the
568 old and the new configuration, respectively. However, during SE winds (Figure 10J), both
569 configurations did not show changes in their total abundance, maintaining approximately 71% (~
570 5000) in the old and approximately 86% (~6000) in the new configuration, with an advance of
571 larvae to area A4.

572 From day 4 (Figure 10E, 10K, 10Q) onward, the new configuration followed the same decay
573 behavior, similar to the old configuration for the SW and S wind. The southern areas of the estuary
574 (A1, A2, and A3), showed low and/or almost no larvae and higher concentrations in the northern
575 areas (A5 and A6) (Figure 10E, 10F, 10K, 10L), demonstrating that part of the larvae may have
576 crossed the northern limit of area A6 (Figure 1C) because, as illustrated in Figure 6, the maximum
577 range of the larvae during the simulated winds exceeded 75 km (northern limit of area A6). The
578 total abundance on the 4th and 5th days decreased to approximately 23% (~1600) in the old
579 configuration and approximately 59% (~4100) in the new configuration during the SW wind, and
580 approximately 44% (~3000) for both configurations during S wind. Larvae during the SE wind only
581 reached the northern limit of the estuary (area A5) on day 5 (Figure 10R) in the new configuration.
582 The total larvae abundance was approximately 93% (~ 6500) and approximately 90% (~ 6300) in
583 the old and new configuration, respectively, and the greatest abundance was concentrated in areas
584 A4 and A5.

585 3.6. Lateral Stratification at the mouth of the estuary

586 3.6.1. Changes on Salinity Stratification

587 The lateral stratification between the jetties was analyzed only for low discharge
588 experiments because at the beginning of the experiments, the plume of the Patos Lagoon was in the
589 adjacent coastal region, allowing the lateral stratification process to be more evident between the
590 jetties (António et al., submitted). The lateral stratification varied from the old (Figure 11A, 11B,
591 11C) to the new (Figure 11D, 11E, 11F) configuration for each incident wind direction. The lateral
592 stratification was more evident during the incidence of the SW wind, both for the old and the new
593 configuration. The beginning of the flood, and consequently the establishment of lateral
594 stratification in both the old and in the new configuration of the Barra Jetties, occurred 1 hour after
595 the beginning of the experiment (Figures 11A and 11D). In the SW wind experiment, the highest
596 salinity was observed near the east jetty and the lowest near the west jetty, both in the old and the
597 new configuration. In the new configuration, however, the salinity gradient was smaller, as the
598 difference in salinity between the east and west was 2.5 psu, while in the old configuration this
599 difference was 5 psu.

600 With the S wind experiment, a clear pattern of lateral stratification was not observed in the
601 two configurations of the Barra Jetties. It should be noted that in the old configuration (Figure 11B)
602 the lateral stratification between the jetties was not established, but the flow of saltwater was
603 present between the jetties 7 hours after the beginning of the experiment, dominating the entire
604 navigation channel. In the new configuration (Figure 11E) at 7 hours, the stratification had not been



605 established, observing the beginning of the entry of saline water from the coastal region into the
606 mouth of the jetties. In the old configuration, the highest salinity was observed more centralized,
607 decreasing for the jetties (Figure 11B). During the SE wind, the lateral stratification was observed
608 only 10 hours after the beginning of the experiment with the highest salinity in the east jetty (Figure
609 11C). In the new configuration, 10 hours after the beginning of the experiment, the navigation
610 channel still did not have lateral stratification (Figure 11F). In general, the beginning of floods and
611 consequently the establishment of lateral stratification occurred faster in the old than in the new
612 configuration, resulting in a difference of 2 hours during S winds and 5 hours during SE winds.

613 3.6.2. Larvae Distribution

614 Analyzing the larvae abundance among the jetties (Figure 12), the dispersion results
615 corroborate with the salinity gradient (Figure 11). During SW winds (Figure 12A, 12D, 12G),
616 stratification was observed 1 h after the beginning of the experiment for both configurations. In the
617 old configuration, the largest number of larvae was concentrated at the root of the jetties, spreading
618 from the central channel toward the east jetty region (Figure 12A). In the new configuration, despite
619 stratification also occurring 1 hour after the beginning of the experiment, the largest number of
620 larvae was concentrated in the center of the jetties, in the east jetty region (Figure 12D). During the
621 S wind (Figure 12B, 12E, 12H), the stratification occurred after 7 hours of simulation. In the old
622 configuration, the largest number of larvae was observed in the mouth of jetties in the central
623 channel region (Figure 12H), concentrating the largest number of larvae in the east jetty and
624 decaying to the west jetty during transport to the interior of the estuary (Figure 12B and 12E). In the
625 new configuration, the larvae were observed only in the region of the mouth of the jetties in the
626 central channel of the jetties (Figure 12H). During the SE wind (Figure 12C, 12F, 12I), the
627 stratification occurred 10 hours after the beginning of the experiment. In the old configuration, the
628 largest number of larvae was observed in the mouth region in the central channel of the jetties
629 (Figure 12I), decreasing linearly from the west to the east jetty during transport to the interior of the
630 estuary (Figure 12C and 12F). In contrast, in the new configuration, no larvae were recorded
631 between the jetties 10 h after the beginning of the experiment (Figure 12I).

632 4. DISCUSSION

633 The present study analyzes the effects of changes in the configuration of coastal structures in
634 the transport and dispersion of eggs and larvae of the croaker, *Micropogonias furnieri*. The study
635 analyzed the case of the Barra Jetties on the access channel to the Patos Lagoon in southern Brazil.
636 Continental discharge and wind are the forces that control circulation in the Patos Lagoon estuary
637 (Moller et al., 2001; Fernandes et al., 2005; Moller and Fernandes, 2010; Odebrecht et al., 2010).
638 The analysis considered two extreme discharge conditions, high in 2003 (El Niño) and low in 2012
639 (La Niña), which reflect the extreme circulation conditions (Moller et al., 2001; Marques and
640 Möller, 2009) and consequently influence the transport of fish eggs and larvae (Muelbert and Weiss,
641 1991). Situations with winds from the south quadrant were simulated because they favor the entry
642 of saltwater (Hartmann and Schettini, 1991; Moller et al., 2001; Moller and Fernandes, 2010;
643 Marques et al., 2011) and consequently maximize the transport of marine organisms to the estuary
644 (Muelbert and Weiss, 1991). In each of these situations, only changes in depth and jetty shape were
645 simulated, which were induced by humans in the project to change the jetties at the entrance to the
646 Patos Lagoon estuary. The duration of 5 days of the experiments, with a continuous incidence of
647 south winds, was defined according to the passage of cold fronts in the region (Moller and
648 Fernandes, 2010), and because it represents the life span of the croaker in which they are passive or
649 do not yet present active movement (Weiss, 1981).

650 Differences, both in saltwater intrusion and in the pattern of transport and dispersal of larvae
651 to the interior of the estuary, were observed between the old and the new configuration of the jetties
652 in the different scenarios analyzed. According to Dugan et al. (2011), the design and inclusion of



653 engineering structures in coastal environments alter hydrodynamics, modifying water flow, wave
654 regime and propagation, sediment dynamics, grain size, and depositional processes. Despite the use
655 of coastal structures around the world for thousands of years, studies on the physical, environmental
656 and economic effects of these structures in open and sheltered coastal regions are recent (Yuk and
657 Aoki, 2007; Azarmsa et al., 2009; Cunha and Caliar, 2009; Ghashemizadeh and Tajziehchi, 2013;
658 Lisboa and Fernandes, 2015; Silva et al., 2015; Prumm and Iglesias, 2016;).

659 Recent jetty modernization works have reduced the incursion of eggs and larvae into the
660 estuary in the new configuration compared to the old jetty configuration. The ecological effects
661 resulting from the construction of these structures have been little studied and understood, and even
662 less about how they alter the functions and services of these natural ecosystems (NRC, 2007;
663 Dugan et al., 2011;). The morphology of the Patos Lagoon mouth plays a fundamental role in the
664 transport and dispersion of eggs (Martins et al., 2007). As a consequence, the larvae took longer to
665 be transported from one area to another as the incursion into the estuary occurred. In this context,
666 the transport of fish eggs and larvae to estuarine breeding sites is important to ensure the
667 recruitment and maintenance of fishing resources (Castro et al. 2005; Vieira et al. 2010;). According
668 to Robins et al., (2013) the larval transport pattern, whether promoting self-recruitment (retention)
669 or high connectivity among local populations, is fundamentally important for species that live in
670 irregular habitats, such as reefs, zones between tides or estuaries.

671 The differences observed in the pattern and extension of larvae incursion in the Patos
672 Lagoon estuary may be due to differences in the bathymetry of the access channel, symmetry and
673 length of the jetties between the two configurations, as well as the convergence and funneling of the
674 jetties in the new configuration (Cunha and Caliar, 2009; Lisboa and Fernandes, 2015). As noted
675 by António et al. (submitted) and Silva et al. (2015), the recent modernization works changed the
676 hydrodynamics of the estuary, reducing saline intrusion as well as the intensity of flood and ebb
677 currents by approximately 20%, along the access channel between the jetties. Such factors harm the
678 flood flows that are responsible for the transport of eggs and larvae in their passive phase to the
679 interior of the estuary (Castro et al., 2005; Martins et al., 2007; Franzen et al., 2019).
680 Complementarily, a partial centralization of the flow along the navigation channel occurred
681 (António et al., Submitted), opposing the previous behavior in which the east jetty was more
682 dynamic than the west jetty (Cunha and Caliar, 2009), which can cause different residual currents
683 as observed in the Aransas Pass estuary in the Gulf of Mexico, implying the transport of eggs and
684 larvae (Brown et al., 2000). Human interventions in estuarine geomorphology lead to changes in the
685 natural flow of saltwater, leading to the loss of habitat and disturbing the ecocline,(which may be
686 the limit between freshwater-oligohaline (upper), between mesohaline-mixoeuhalina (medium) and
687 between euhaline-hyperhaline (lower reaches)) throughout the estuarine system, preventing the fish
688 from moving between previously connected habitats, especially in the previous ontogenetic phases
689 (Barletta and Lima, 2019). The results of the study demonstrated that the influence of the local
690 geomorphology in the variation of circulation conditioned the way that the fish larvae are
691 transported to the estuary, a crucial parameter when associated with other physical and biological
692 factors that are determinant for transport during the initial stage of life of the larvae (Able, 2005;
693 Barletta and Lima, 2019). The factors mentioned also affected the larvae trajectory, and differences
694 were observed in the estuary between the two configurations. It was also found that at the end of
695 each day, the average distances traveled were shorter in the new configuration of the jetties. Costa
696 et al. (2013) analyzed studies carried out in the Mondego estuary and found that in the last decades,
697 the estuaries have suffered intense anthropic pressure and hydromorphological changes that have
698 led to a progressive decline in their ecological condition, leading to continuous degradation of the
699 ecosystem.

700 The number of larvae that entered the estuary also differed between the old and the new jetty
701 configuration. The change in the configuration of the jetties resulted in differentiated transport to
702 the interior of the estuary. The abundance of eggs in the access channel was higher in the old



703 configuration 1 hour after the beginning of the experiment, a trend that remained from area to area
704 until the final location of the larvae at the end of the experiment. Combined with the reduction of
705 flood currents along the navigation channel, the reduction of the cross-sectional area by
706 approximately 15% (due to the change in the mouth configuration), despite the increase in depth by
707 approximately 2 m (Antônio et al., submitted; Silva et al., 2015) and the extension of the jetties
708 after the recent works, may be limiting and/or hindering the incursion of the larvae passively
709 transported to the estuary. Moreover, increasing or decreasing the current velocities has a direct
710 impact on the transport of particles and water properties that depend on it (Castro et al., 2005 ;
711 Cunha and Caliarí, 2009). However, in the Patos Lagoon, eggs and larvae of species such as croaker
712 enter the estuary with the intrusion of saltwater from the adjacent coastal region where the species
713 spawns (Castello, 1986; Sinque and Muelbert, 1997; Vieira and Castello 1997; Odebrecht et al.
714 2017).

715 The reduced incursion caused by the delay in the entry of eggs and larvae into the estuary in
716 the new configuration of the jetties will contribute to a greater loss due to their dispersion in the
717 adjacent coastal region. The reduction in the number of organisms that enter the estuary, which is a
718 nursery (Odebrecht et al. 2017) and contains more appropriate conditions for development, could
719 result in negative conditions for the croaker population. Ramos et al. (2006) found that
720 environmental parameters such as increased river flow can prevent the recruitment of marine
721 species, leading to a decrease in diversity in the estuarine region as well as variations in abundance,
722 total diversity, and in the structure of the larval fish assembly, as observed in the Lima estuary. In
723 the coastal region adjacent to the study, ocean currents, tides, and meteorological conditions are the
724 main forces responsible for the transport and dispersion of organisms (Acha et al., 2004; Muelbert
725 et al., 2008). Environments with high tidal energy and high variability in oceanographic conditions,
726 such as coastal regions, lead to greater dispersion of larvae to places far from the population
727 (Robins et al., 2013) as well as to areas with conditions that are not appropriate for their
728 development such as the open sea. Although unfavorable environmental conditions rarely directly
729 induce larval mortality, they contribute indirectly, prolonging the planktonic phase, so that the
730 larvae are more exposed to planktonic dispersion, predation, or lack of food (Ellien et al., 2004). In
731 this sense, hydrodynamics has a fundamental role in the planktonic phase, impacting larval
732 mortality as found by Ellien et al. (2004), where the weak residual currents in the east of the Sena
733 Bay contributed to the increase in mortality of *Pectinaria koreni* by reducing the duration of its
734 larval life stage. Therefore, Araujo et al., (2016) analyzed samples of organisms in Sepetiba Bay for
735 periods covering 3 decades and found significant differences in the structure of fish communities, as
736 the number of species, individuals and families have changed and/or decreased in the inner and
737 intermediate bay. Such findings demonstrate that anthropic changes can lead to a reduction in the
738 incursion, structure, and composition of organisms in the estuary.

739 Furthermore, regarding the distance and the quantity, the maximum (final) reach of the
740 larvae incursion inside the estuary was also reduced in the new configuration of the jetties at both
741 high and low discharge. In the low discharges, there was a greater incursion and reach of the larvae
742 to the interior of the estuary, which can minimize losses by ensuring that the larvae enter the estuary
743 during periods with weak currents (toward the coastal) because the greater water volume in the
744 estuary, observed normally during El Niño, needs greater flow or time for its outflow, while the
745 opposite is observed with low flow favoring the input of saltwater into larger areas of the lagoon, a
746 condition commonly observed in southern Brazil (Acha et al. 1999; Odebrecht et al. 2017). The
747 differences in the daily distances covered revealed that the maximum (final) distance reached by the
748 salinity and the larvae at the end of the 5 days was smaller in the new configuration. The reduced
749 incursion is a response to the effect of the reduced entrance area at the mouth, associated with the
750 weak currents that transported the larvae along the access channel in the new configuration
751 compared to the old jetty configuration. A reduced penetration of the organisms will result in the
752 reduction of the oligohaline limit and in the diversity of organisms in distances previously observed,



753 which will change the structure and composition of the fauna and the environment inside the
754 estuaries. This may directly reveal the observation and occurrence of organisms of estuarine-
755 dependent species further north of the estuary over distances previously recorded. Odebrecht et al.
756 (2005) found that the reduced limit of the salinity range reduces the oligohaline region of the Patos
757 Lagoon, an important characteristic for the distribution of species and biodiversity. However, the
758 reduced distances traveled by the larvae in the new configuration, reflecting the reduced saline
759 intrusion, may interfere with the number of larvae considering a continuous entry into the estuary,
760 given that, as argued by Able (2005), a stronger salinity gradient at the estuary-ocean interface may
761 prove to be a major barrier in terms of quantity for the use of larvae and juvenile fish in these
762 habitats. Fish wealth and abundance have decreased in the last three decades (1990–2010) in
763 Sepetiba Bay, and more pronounced changes have been observed in the inner and middle bays,
764 noting that changes in the salinity gradient have led to spatial changes in fish communities due to
765 the expansion of the port (Araújo et al., 2017). Such port expansion activities, which included
766 dredging to deepen the navigation channel, contribute to the degradation of the coast, the
767 impoverishment of natural habitats, and an increase in the pollutant load in the bay.

768 The circulation observed among the jetties in the access channel to the Patos Lagoon forces
769 the establishment of lateral stratification, a pattern that was also observed in the access channel to
770 the bay of Aransas Pass (Bown et al., 2000; Cunha and Calari, 2009; Marques et al., 2011). The
771 recent jetty modernization works have also affected the establishment of lateral stratification in
772 periods of low discharge. A delay in the time of occurrence of lateral stratification was recorded in
773 the new configuration of the jetties, implying a decrease in the number of eggs and larvae
774 transported during the incidence of SW and S winds, and the non-entry of eggs and larvae during
775 the SE wind in the access channel to the estuary. The effect that coincides with the weak flood
776 currents caused by the change in the configuration of the mouths of the jetties (Antônio et al,
777 submitted; Silva et al. 2015) is due to the asymmetry in the length of the jetties (Cunha and Calari,
778 2009; Moller and Fernandes, 2010). A similar result was found on the jetties at Aransa Pass (Bown
779 et al., 2000). In contrast to what happened in the bay of Aransas Pass, in the Patos Lagoon, the
780 asymmetry of the jetties was intense in the old configuration. What justifies the delay in the start
781 time of the occurrence of lateral stratification, combining symmetry and the increase in the length of
782 the jetties in the new configuration, which results in the reduction of the intensity of the currents
783 between the jetties (Antônio et al., Submitted; Silva et al 2015). In this way, it is expected that the
784 location that holds the highest concentrations of eggs and larvae will be altered as consequence of
785 the reduction in the daily distance and the maximum extent covered by the eggs and larvae toward
786 the interior of the estuary. During the lateral stratification between the jetties, each incident wind
787 presented a specific characteristic in the larvae distribution pattern during the incursion into the
788 estuary and the location of greater concentration in the new configuration did not change
789 significantly; however, there is still a need for further analysis since the lateral stratification was not
790 fully established in the time observed for the old configuration for the 3 winds studied. This fact
791 meant that the variations in the region with the highest concentration of eggs and larvae observed
792 were mainly determined by the direction of the incident wind. Dugan et al. (2011) and Moller and
793 Fernandes (2010) believe that the deepening and narrowing of the tidal channels that result from the
794 shielding, channeling and construction of jetties and coastal infrastructure have been associated
795 with the vertical modification of stratification and the increase or decrease in the penetration of
796 saltwater and hypoxia in urbanized estuaries, a fact that contributes to the destruction of the ecology
797 of coastal and estuarine ecosystems.

798 Despite the lack of statistical significance regarding the differences observed between the
799 old and the new configuration of the Barra Jetties, they suggest a reduction in the entry of eggs and
800 larvae of the estuarine-dependent organisms, which may aggravate the problem of the decay of
801 species diversity and abundance. This decay may result in a reduction in the stock of adults and,
802 consequently, in the fishing stock, which already has losses in the coastal region (Haimovici and



803 Cardoso, 2017; Odebrecht et al., 2017) since the estuary is the most suitable place for guaranteed
804 retention that enables completing the phases of their life cycle (Acha et al., 1999; Muelbert et al.,
805 2008).

806 Figure 13 presents the conceptual model of eggs and larvae transport during the incidence of
807 southern winds (SW, S, and SE) for the old and the new configuration of the Barra Jetties. The
808 transport and dispersion of eggs and larvae in the first moments after the start of the simulations are
809 forced by the pattern of velocity currents in the coastal region (Figure 13A, 13B, and 13C), which
810 are determined by the direction of the incident wind. In the experiments in both configurations, re-
811 circulation zones with turns are formed at the root of the west jetty, a place that can concentrate and/
812 or retain larvae in the central region of the turns, both cyclonic and anti-cyclonic, due to the
813 trapping conditions in the protected region. The coastal circulation forms lines of currents that
814 skirted the jetties which, depending on the wind, favor the transport of organisms to the interior of
815 the estuary. The contribution of these physical conditions conditioned the differentiated transport of
816 eggs and larvae (Figure 13D). The differences in the jetty configurations determined the extension
817 of penetration and abundance of eggs and larvae within the estuary. A shorter incursion time and a
818 greater range and concentration of larvae stood out in the old configuration, while in the new
819 configuration, a delay in stratification time, a reduction of the maximum incursion, and the
820 concentration of larvae were registered.

821 5. CONCLUSION AND REMARKS

822 The study results demonstrated that the recent modernization works of the Barra Jetties of
823 the Rio Grande affected the extension of recruitment incursion, the abundance, and the distribution
824 of eggs and larvae observed in 2003 (El Niño) and 2012 (La Niña). A reduction in these indices was
825 notable in the new configuration when compared to the old configuration, during the transportation
826 into the estuary with SW, S and SE incident winds. The recent modernization works also changed
827 the time for the start of lateral stratification and how the eggs and larvae enter the estuary, with a
828 delay in the new configuration for the 3 simulated winds (SW, S, SE).

829 The present study concludes, therefore, that the differences in transport, the dispersion of
830 eggs and larvae to the Patos Lagoon, and the extension and its variability are attributed to
831 hydrodynamic factor changes caused by changes in the geomorphology of the estuarine
832 environment imposed by the jetty configuration changes. However, considering the limitations of
833 the results of the TELEMAC-3D model, and taking into account the complexity of the study in this
834 initial phase of the life cycle of the *Micropogonias furnieri* species, this information serves as a first
835 response to the problem of declining abundance and capture of the adult stock in the Patos Lagoon
836 estuary. Therefore, future work is necessary to continue the investigations and will include studying
837 the biological and behavioral characteristics of the species, such as growth rate, temperature, and
838 mortality, which are fundamental factors for the real dimension of successful recruitment.

839 ACKNOWLEDGMENTS

840 The authors would like to acknowledge CAPES (*Coordenação de Aperfeiçoamento Pessoal*
841 *de Ensino Superior*) for sponsoring the first author's (MHA) PhD's grant through the *Programa de*
842 *Pós-Graduação Ciência para o Desenvolvimento* (PGCD), and provided resources support to the
843 Postgraduate Program in Oceanology. We thank the CNPq (*Conselho Nacional de Desenvolvimento*
844 *Científico and Tecnológico*) for the research grants 308274/2011-3 (EHF) and Proc. 310047/2016-1
845 (JHM). This study was partially funded by the Brazilian Long-Term Ecological Research Program
846 (PELD) from CNPq (Proc.441492/2016-9) and the Fundação de Amparo à Pesquisa do Estado do
847 Rio Grande do Sul (Proc. 16/2551-0000102-2). We are also grateful to the LOCOSTE (*Laboratório*
848 *de Oceanografia Costeira e Estuarina*) team for giving support during this research and to Prof. Dr.
849 Osmar Moller for providing the in situ data used to calibration and validation of TELEMAC-3D
850 model.



851 REFERENCES

- 852 Able, K.W. A re-examination of fish estuarine dependence: evidence for connectivity between estuarine and ocean
853 habitats. *Estuarine, Coastal and Shelf Science* 64 (1): 5–17. <https://doi.org/10.1016/j.ecss.2005.02.002>, 2005.
- 854 Acha, E. M., Mianzan, H., Guerrero, R., Carreto, J., Giberto, D., Montoya, N. and Carignan, M. An overview of
855 physical and ecological processes in the Rio de la Plata Estuary. *Continental Shelf Research*. Volume 28, Issue
856 13, Pp.1579-1588. [Doi.org/10.1016/j.csr.2007.01.031](https://doi.org/10.1016/j.csr.2007.01.031), 2008.
- 857 Acha, E.M., Simionato, C.G., Carozza, C., Mianzan, H. Climate-induced year-class fluctuations of whitemouth croaker
858 *Micropogonias furnieri* (Pisces, Sciaenidae) in the Rio de la Plata estuary, Argentina–Uruguay. *Fish. Oceanogr.*
859 21 (1), 58–77, 2012.
- 860 Acha, E. M., Mianzan, H., Lasta, C. A. and Guerrero, R. A. Estuarine spawning of the whitemouth croaker
861 *Micropogonias furnieri* (Pisces: Sciaenidae), in the Río de la Plata, Argentina. *Mar. Freshwater Research*. 50,
862 57-65. DOI: 10.1071/MF98045, 1999.
- 863 Albuquerque, C. Q. Bionomia da corvina *Micropogonias furnieri* no extremo sul de sua área de ocorrência, através
864 da análise química de otólitos. Ph.D Teses. Programa de Pós-Graduação em Oceanografia Biológica.
865 Universidade Federal do Rio Grande, Rio Grande, RS. Brasil, 2008.
- 866 Albuquerque, C. Q., Muelbert, J. H. and Sampaio, L. A. N. Early developmental aspects and validation of daily
867 growth increments in otoliths of *Micropogonias furnieri* (Pisces, Sciaenidae) larvae reared in the laboratory. *Pan-*
868 *American Journal of Aquatic Sciences*, 4(3): 259-266, 2009.
- 869 Antônio, M. H. P., Fernandes, E. H. and Muelbert, J. H. Impact of jetties configuration changes on the
870 hydrodynamics of the subtropical Patos Lagoon Estuary, Brazil, Submitted.
- 871 Araújo, G. F., Azevedo, M. C. C. Guedes, A. P. P. Inter-decadal changes in fish communities of a tropical bay in
872 southeastern Brazil. *Regional Studies in Marine Science*. <http://dx.doi.org/10.1016/j.rsm.2015.06.001>, 2016.
- 873 Araújo, F. G., Pinto, S. M., Neves, L. M., Azevedo, M. C. C. Inter-annual changes in fish communities of a
874 tropical bay in southeastern Brazil: What can be inferred from anthropogenic activities? *Marine Pollution*
875 *Bulletin*, 114(1), 102–113. DOI:10.1016/j.marpolbul.2016.08.063, 2017.
- 876 Azarmsa, S. A., Esmaili, M. and Khaniki, A. K. Impacts of Jetty construction on the wave heights of the Kiashahr
877 lagoon. *Aquatic Ecosystem Health & Management*, 12(4):358-363. ISSN: 1463-4988. DOI:
878 10.1080/14634980903354726, 2009.
- 879 Barletta, M., and Lima, A. R. A. Systematic Review of Fish Ecology and Anthropogenic Impacts in South
880 American Estuaries: Setting Priorities for Ecosystem Conservation. *Frontiers in Marine Science*, Vol. 6:237.
881 DOI: 10.3389/fmars.2019.00237, 2019.
- 882 Blanton, J. O., Werner, F. E., Kapolnai, A., Blanton, B. O., Knott, D. and Wenner, E. L. Wind-generated transport of
883 fictitious passive larvae into shallow tidal estuaries. *Fish. Oceanogr.* 8(Suppl. 2), 210-223, 1999.
- 884 Brown, C. A., Jackson, G. A. and Brooks, D. A. Particle transport through a marraw tidal inlet due to tidal
885 forcing and implications for larval transport. *Journal of Geophysical Research*, Vol. 105, nº C10, Pag, 141-24,
886 156, 2000.
- 887 Bruno, M. A. and Muelbert, J. H. Distribuição Espacial e Variações Temporais da Abundância de Ovos e Larvas de
888 *Micropogonias Furnieri*, no Estuário da Lagoa dos Patos: Registros Históricos e Forçantes Ambientais.
889 *Atlantica*, Rio Grande. 51-68. doi: 10.5088/atl. 2009.31.1.51, 2009.
- 890 Castello, J. P. Distribución, crecimiento y maduración sexual de la corvina juvenil (*Micropogonias furnieri*) en el
891 estuario de la ‘Lagoa dos Patos’, Brasil. *Physis* 44, 21-36, 1986.
- 892 Castro, M. S., Bonecker, A. C. T., and Valentin, J. L. Seasonal Variation in Fish Larvae at the Entrance of Guanabara
893 Bay, Brazil. *Brazilian Archives of Biology And Technology*. Vol. 48, n.1, pp. 121-128, ISSN 1516-8913, 2005.
- 894 Cochran, W. G. *Samplig Techniques*. Third edition. By John Wiley and Sons, Inc., 1977. ISBN 0-471-16240-X. Pp.
895 77-728, 1976.
- 896 Costa, S., Azeiteiro, U. M., and Pardal, M. A. The contribution of scientific research for integrated coastal management:
897 The Mondego estuary as study case. *Journal of Integrated Coastal Zone Management* 13(2):229-241.
898 DOI:10.5894/rgci391, 2013.
- 899 Costa, M. D. P., Muelbert, J. H., Moraes, L. E., Vieira, J. P. and Castello, J. P. Estuarine early life stage habitat
900 occupancy patterns of whitemouth croaker *Micropogonias furnieri* (Desmarest, 1830) from the Patos Lagoon,
901 Brazil. *Fisheries Research* 160. Pp. 77–84. <http://dx.doi.org/10.1016/j.fishres.2013.10.025>, 2014.
- 902 Cunha, R. M. P. and Calliari, L. J. Natural and antropic geomorphological changes in the inlet of Patos Lagoon
903 before and after its fixation. *Journal of Coastal Research*, SI 56 (Proceedings of the 10th International Coastal
904 Symposium), 708 – 712. Lisbon, Portugal, ISSN 0749-0258, 2009.
- 905 D’Incao, F. Pesca e biologia de *Penaeus paulensis* na Lagoa dos Patos, RS. *Atlântica*, Rio Grande, 13(1): 159-169, 1991.
- 906 Dugan, J. E., Airolidi, L., Chapman, M. G., Walker, S. J. and Schlacher, T. Estuarine and Coastal Structures:
907 Environmental Effects, A Focus on Shore and Nearshore Structures. *Treatise on Estuarine and Coastal Science*,
908 2011, Vol.8, 17-41, DOI: 10.1016/B978-0-12-374711-2.00802-0, 2011.
- 909 Ellien, C., Thiébaud, E., Dumas, F., Salomon, J-C. and Nival, P. A modeling study of the respective role of
910 hydrodynamic processes and larval mortality on larval dispersal and recruitment of benthic invertebrates:



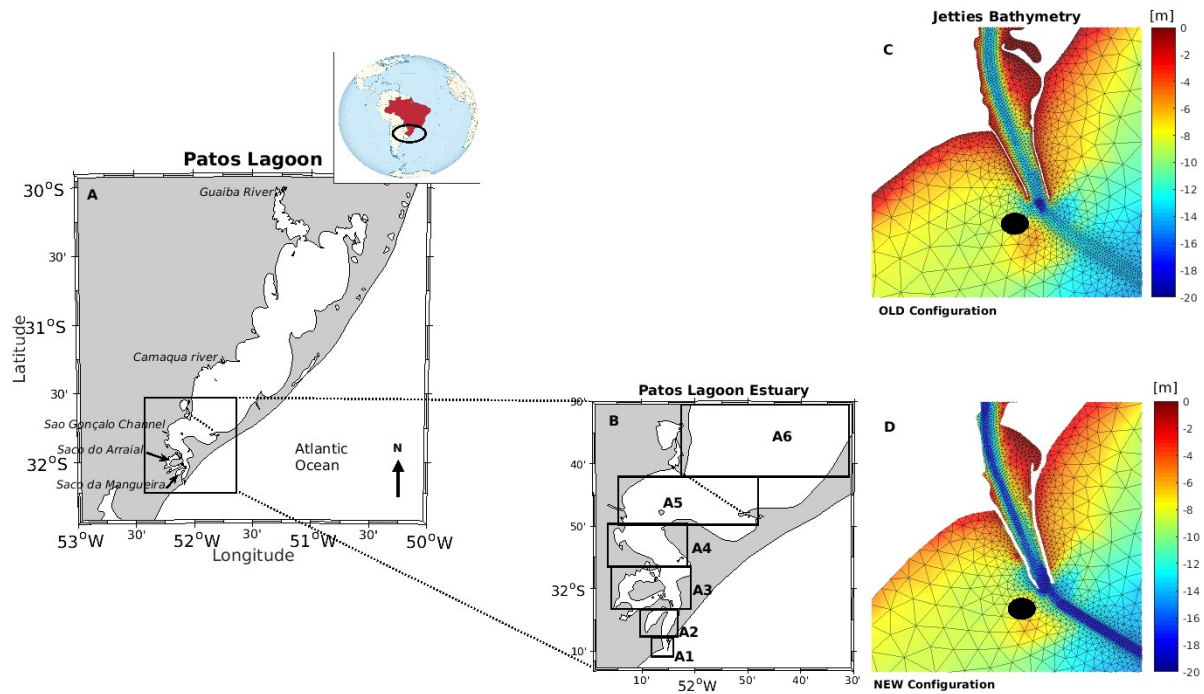
- 911 example of *Pectinaria koreni* (Annelida: Polychaeta) in the Bay of Seine (English Channel). *Journal of*
912 *Plankton Research* Vol. 26 No. 2, Pp. 117-132. DOI: 10.1093/plankt/fbh018, 2004.
- 913 Endo, C. A. K., Gherardi, D. F. M., Pezzi, L.P. and Lima L. N. Low connectivity compromises the conservation of reef
914 fishes by marine protected areas in the tropical South Atlantic. *Nature, Scientific Reports*, 9:8634.
915 <https://doi.org/10.1038/s41598-019-45042-0>, 2019.
- 916 Fernandes, E. H. L., Dyer, K. R. and Moller, O. O. Spatial Gradients in Flow of Southern Patos Lagoon. *Journal of*
917 *Coastal Research*, 21(4), 759-769, West Palm Beach (Florida), ISSN 0749-0208, 2005.
- 918 Franzen, M. O., Muelbert, J. H. and Fernandes, E. H.. Influence of wind events on the transport of early stages of
919 *Micropogonias furnieri* (Desmarest, 1823) to a subtropical estuary. *Latin American Journal of Aquatic Research*,
920 47(3): 536 -546. DOI: 10.3856/vol47-issue3-fulltext-15, 2019.
- 921 Garcia, A. M., Vieira, J. P. and Winemiller, K.O. Dynamics of the shallow-water fish assemblage of the Patos
922 Lagoon estuary (Brazil) during cold and warm ENSO episodes. *Journal of Fish Biology*. 59:1218-1238, 2001.
- 923 George, G., Vethamony, P., Sudheesh, K. and Babu, M. T. Fish larval transport in a macro-tidal regime: Gulf of
924 Kachchh, west coast of India. *Fisheries Research* 110. Pp. 160–169. doi:10.1016/j.fishres.2011.04.002, 2011.
- 925 Ghashemizadeh, N. and Tajziehchi, M. Impact of Long Jetty on Shoreline Evaluation (Case Study: Eastern
926 Coast of Bandar Abbas). *Journal of Basic and Applied Scientific Research*. ISSN 2090-4304,Pp 1256-
927 1266, 2013.
- 928 Haimovici, M. and Cardoso, L. G. Long-term changes in the fisheries in the Patos Lagoon estuary and adjacent coastal
929 waters in Southern Brazil, *Marine Biology Research*, 13:1, 135-150. DOI: 10.1080/17451000.2016.1228978,
930 2017.
- 931 Hartmann, C., and Schettini, C. A. F. Aspectos hidrológicos na desembocadura da Laguna dos Patos, RS, *Rev. Bras.*
932 *Geocienc.*, 21, 371–377, 1991.
- 933 Hervouet, J. M. *Hydrodynamics of Free Surface Flows: Modeling with the Finite Element Method*, Wiley,
934 Chichester, 2007.
- 935 Hinrichsen, H-H. Biological processes and links to the physics. *Deep-Sea Research II* 56. Pp. 1968–1983.
936 doi:10.1016/j.dsr2.2008.11.008, 2009.
- 937 Houde, E. D. Emerging from Hjort's Shadow. *J. Northw. Atl. Fish. Sci.*, 41: 53–70. DOI:10.2960/J.v41.m634, 2008.
- 938 Ibagy, A. S. and Sinque, C. Distribuição de ovos e larvas de Sciaenidae (Perciformes-Teleostei) da região costeira do
939 Rio Grande do Sul-Brasil. *Arquivos Biologia e Tecnologia* 38 (1), 249–270, 1995.
- 940 Israel, G. D. Determining Sampling Size. IFAS Extension. PEOD6. University of Florida, 1992.
- 941 Joyeux, J-C. The retention of fish larvae in estuaries: among-tide variability at Beaufort Inlet, North Carolina, USA.
942 *Journal Mar. Biol. Ass. U.K.* (81), Pp 857-868, 2001.
- 943 Kjerfve, B. and Magill, K.E.. Comparative oceanography of coastal lagoons, p. 63-81. In: Wolfe, D. A. ed. *Estuarine*
944 *variability*. New York, Academic Press. 509P, 1986.
- 945 Lisboa, P. V. and Fernandes, E. H. Anthropogenic influence on the sedimentary dynamics of a sand spit bar, Patos
946 Lagoon Estuary, RS, Brazil. *Journal of Integrated Coastal Zone Management*, 15(1): 35-46. DOI:10.5894/
947 rgci54, 2015.
- 948 Liu, W-C and Chan, W-T. Assessment of Climate Change Impacts on Water Quality in a Tidal Estuarine System Using a
949 Three-Dimensional Model. *Water* 2016, 8, 60; doi:10.3390/w8020060, 2016.
- 950 Louangrath, P. *Common Statistical Tables*. DOI: 10.13140/RG.2.1.2206.5769, 2015.
- 951 Lough, R. G., Smith, W. G., Werner, F. E., Loder, J. W., Page, F. H., Hannah, C. G., Naimie, C. E., Perry, R. I., Sinclair,
952 M., and Lynch, D. R. Influence of wind-driven advection on interannual variability in cod egg and larval
953 distributions on Georges Bank: 1982 vs 1985. - *ICES mar. Sei. Symp.*, 198: 356-378, 1994.
- 954 Marques, W. C., and Möller, O. O. Variabilidade temporal em longo período da descarga fluvial e níveis de água da
955 Lagoa dos Patos, Rio Grande do Sul, Brasil, *Rev. Bras. Recursos Hídricos*, 13, 155-163, 2009.
- 956 Marques, W. C., Fernandes, E. H. L., and Rocha, L. A. O. Straining and advection contributions to the mixing process in
957 the Patos Lagoon estuary, Brazil, *J. Geophys. Res.*, 116, C03016. DOI:10.1029/2010JC006524, 2011.
- 958 Martins, I. M. S., Dias, J. M., Fernandes, E. H. L. and Muelbert, J. H. Numerical modeling of fish eggs dispersion at
959 the Patos Lagoon estuary -Brazil. *Journal of Marine Systems*, 68: 537-555, 2007.
- 960 Miaoulis, G. and Michener, R. D. *An Introduction to Sampling*. Dubuque, Iowa: Kendall/Hunt Publishing
961 Company, 1976.
- 962 Muelbert, J. H. and Weiss, G. Abundance and distribution of fish larvae in the channel area of Patos Lagoon estuary,
963 Brazil. In: NOAA Technical Report NMFS, vol. 95., pp. 43–5, 1991.
- 964 Muelbert, J. H., Acha, M., Mianzan, H., Guerrero, R., Reta, R., Braga, E. S., Garcia, V. M.T. Berasategui, A., Gomez-
965 Erache, M. and Ramirez, F. Biological, physical and chemical properties at the Subtropical Shelf Front Zone
966 in the SW Atlantic Continental Shelf. *Continental Shelf Research*, 28. Pp.1662–1673.
967 DOI:10.1016/j.csr.2007.08.011, 2008.
- 968 Moller, O. O., Castaing, P., Salomon, S. and Lazure, P. The Influence of Local and Non-local Forcing Effects on the
969 Subtidal Circulation Of Patos Lagoon. *Estuaries*, Vol. 24, N°2, p. 297-311, 2001.



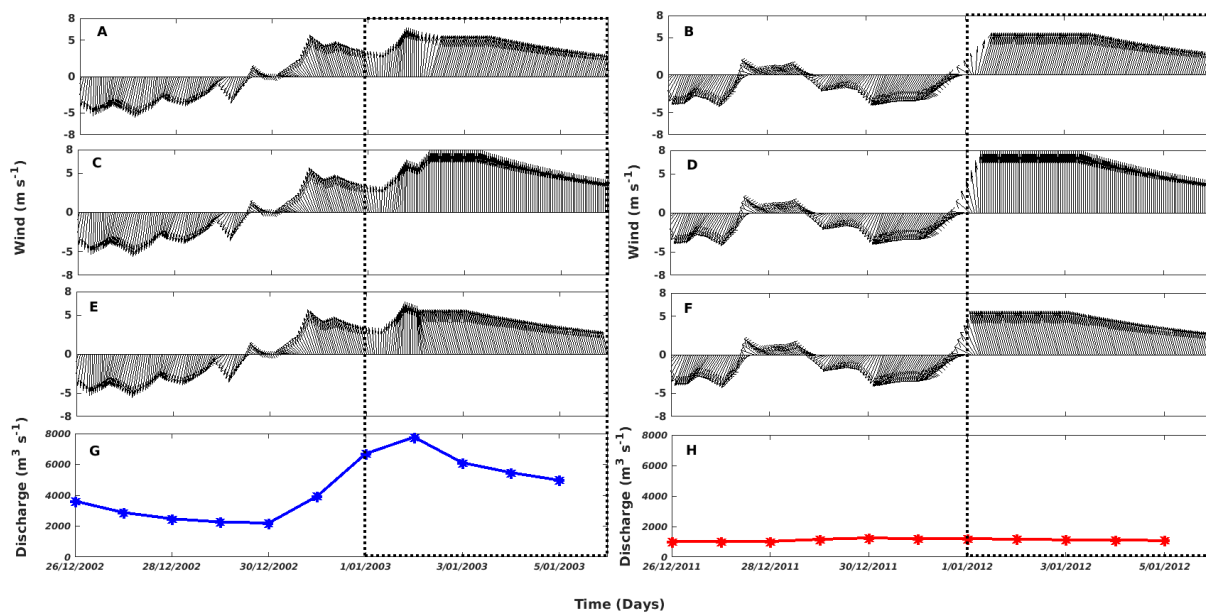
- 970 Moller, O. O., Castello, J. P. and Vaz, A. C. The Effect of river discharge and winds on the interannual variability of the
971 Pink Shrimp *Farfantepenaeus paulensis* Production in Patos Lagoon; Estuaries and Coasts, 787-796. Doi:
972 10.1007/s12237-009-9168-6, 2009.
- 973 Moller, O. O. and Fernandes, E. H. L. Hidrologia e Hidrodinâmica. In: Seeliger, U. and Odebrecht, C (Eds.). O Estuário
974 da Lagoa dos Patos: Um século de transformações. Rio Franque, FURG, P180. ISBN: 978-85-7566-144-4,
975 pp17-27, 2010.
- 976 MPA. Boletim Estatístico da Pesca e Aquicultura – Brasil. Ministério da Pesca e Aquicultura, Brasília, 2011.
- 977 NRC. Mitigating Shoreline Erosion along Sheltered Coasts. Ocean Study Board, National Research Council.
978 National Academies Press, Washington, DC, 2007.
- 979 Odebrecht, C., Bergesch, M., Medeanic, S. and Abreu, P. C. A comunidade de microalgas. In: Seeliger, U. and
980 Odebrecht, C. (Eds.). O Estuário da Lagoa dos Patos: Um século de transformações. Rio Franque, FURG,
981 P180. ISBN: 978-85-7566-144-4, pp 51-63, 2010.
- 982 Odebrecht, C., Secchi, E., Abreu, P. C., Muelbert, J. H., and Uiblein, F. Biota of the Patos Lagoon estuary and
983 adjacent marine coast: long-term changes induced by natural and human-related factors, Marine Biology
984 Research, 13:1, 3-8, DOI: 10.1080/17451000.2016.1258714, 2017.
- 985 Padovani, C. R. Bioestatística. São Paulo: Cultura Acadêmica :Universidade Estadual Paulista, Pró-Reitoria de
986 Graduação, 2012. 112 p. ISBN 978-85-7983-265-9, 2012.
- 987 Prumm, M and Iglesias, G. Impacts of port development on estuarine morphodynamics: Ribadeo (Spain). Ocean and
988 Coastal Management 130, 58-72, 2016.
- 989 Ramos, S., Cowen, R. K., Ré, P., and Bordalo, A. A. Temporal and spatial distribution of larval fish assemblages in the
990 Lima estuary (Portugal). Estuarine, Coastal and Shelf Science 66, 303-314. DOI:10.1016/j.ecss.2005.09.012,
991 2006.
- 992 Robins, P. E., Neill, S. P., Giménez, L., Jenkins, S. R. and Malham, S. K. Physical and biological controls on larval
993 dispersal and connectivity in a highly energetic shelf sea. Limnol. Oceanogr., 58(2), Pp.505–524.
994 DOI:10.4319/lo.2013.58.2.0505, 2013.
- 995 Salvador, N. L. A. and Muelbert, J. H. Environmental variability and body condition of Argentine menhaden
996 larvae, *Brevoortia pectinata* (Jenyns, 1842), in estuarine and coastal waters. Estuaries and Coasts 42,
997 1654–1661. <https://doi.org/10.1007/s12237-019-00604-3>, 2019.
- 998 Seiler, L. M. N., Fernandes, E. H. L., Martins, F. and Abreu, P. C. Evolution of hydrologic influence on water quality
999 variation in a coastal lagoon through numerical modeling. Ecological Modelling 314, 44-61, Elsevier, 2015.
- 1000 Sentchev, A. and Korotenko, K. Modelling distribution of flounder larvae in the eastern English Channel: sensitivity to
1001 physical forcing and biological behaviour. Marine Ecology Progress Series. Vol. 347:233-245. doi:10.3354/
1002 meps06981. 2007.
- 1003 Silva, P. D., Lisboa, P. V. and Fernandes, E. H. 2015. Changes on the fine sediment dynamics after the Port of Rio
1004 Grande expansion. Advances in Geosciences 39, 123–127. DOI:10.5194/adgeo-39-123-2015, 2015.
- 1005 Student (William Sealy Gosset). The probable error of a mean. Biometrika, 6 (1). Pp. 1–25.
1006 doi:10.1093/biomet/6.1.1, 1908.
- 1007 Teodósio, M. A., Paris, C. B., Wolanski, E., Morais, P. Biophysical processes leading to the ingress of temperate fish
1008 larvae into estuarine nursery areas. Estuarine, Coastal and Shelf Science. doi: 10.1016/j.ecss.2016.10.022,
1009 2016.
- 1010 Tiessen, M. C. H., Fernard, L., Gerkema, T., van der Molen, J., Ruardij, P. and van der Veer, H. W. Numerical
1011 modelling of physical processes governing larval transport in the Southern North Sea. Ocean Science Discuss,
1012 10, 1765–1806. doi:10.5194/osd-10-1765-2013, 2013.
- 1013 Torrence, C. and Compo, G. P. A Practical guide of wavelet analyses. Bulletin of the American Meteorological
1014 Society. Vol. 79. nº1. 61-79, 1998.
- 1015 Vaz, A. C., O. O. Möller, and Almeida, T.L. Análise quantitativa da descarga dos rios afluentes da Lagoa dos Patos.
1016 Atlântica, vol. 28, nº 1, pp 13-23, 2006.
- 1017 Vaz, A. C., Parada, C. E., Palma, E. D., Muelbert, J. H. and Campos, E. J. D. Modeling transport and retention of
1018 *Engraulis anchoita* Hubbs & Marini, 1935 (Clupeiformes, Engraulidae) early life stages along the Central
1019 Southwestern Atlantic Continental Shelf. PanAmerican Journal of Aquatic Sciences, 2(2): 179-190, 2007.
- 1020 Vieira, J. P., and Castello, J. P. Environment and biota of the Patos Lagoon Estuary. Fish fauna. In 'Subtropical
1021 Convergence Environments. The Coast and Sea in the Southwestern Atlantic'. Eds U. Seeliger, C. Odebrecht,
1022 and J. P. Castello. pp. 56-61. Springer: Heidelberg, 1997.
- 1023 Vieira, J. P., Garcia, A. and Moraes, L.. A assembleia de peixes. O estuário da Lagoa dos Patos: Um século de
1024 Transformação. Edição: U. Seelinger e C. Odebrecht. FURG. Pp. 79-88, 2010.
- 1025 Walstra, L., Van Rijn, L., Blogg, H. and Van Ormondt, M. Evaluation of a hydrodynamic area model based on the
1026 coast3d data at Teignmouth 1999. p. D4.1–D4.4, 2001.
- 1027 Weiss, G. Ictioplankton del Estuario de Lagoa dos Patos, Brasil. Ph.D Teses. Unversidade Nacional de La Plata.
1028 Uruguai. 164p, 1981.



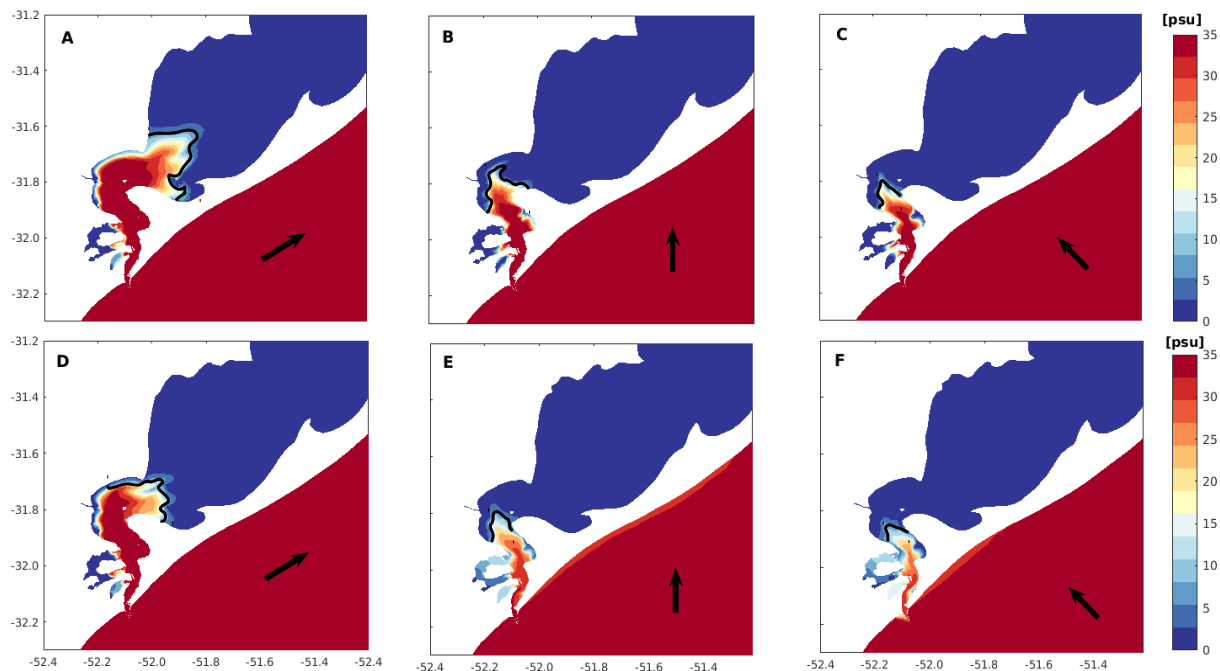
- 1029 Whitfield, A. K. The role of seagrass meadows, mangrove forests, salt marshes and reed beds as nursery areas and food
1030 sources for fishes in estuaries. *Rev. Fish Biol. Fisheries*, Springer. Doi: 10.1007/s11160-016-9454-x, 2016.
1031 Yuk, J. H. and Aoki, S. Impact of Jetty construction on the current and Ecological Systems in the Estuary with a
1032 Narrow Inlet. *Journal of coastal research*, 784-788, 2007.



1033 Figure 1: The study site located in Southeast South America, depicting the Patos Lagoon (A) and
1034 the estuary (B). Dotted line indicates the estuarine limit (Ponta da Feitoria). Five rectangles areas
1035 (A1 – A5) show the location where the model concentration results were extracted. The lower Patos
1036 Lagoon estuary in the (C) old, and (D) new jetty configuration. Black points indicate the position
1037 where the eggs were released.

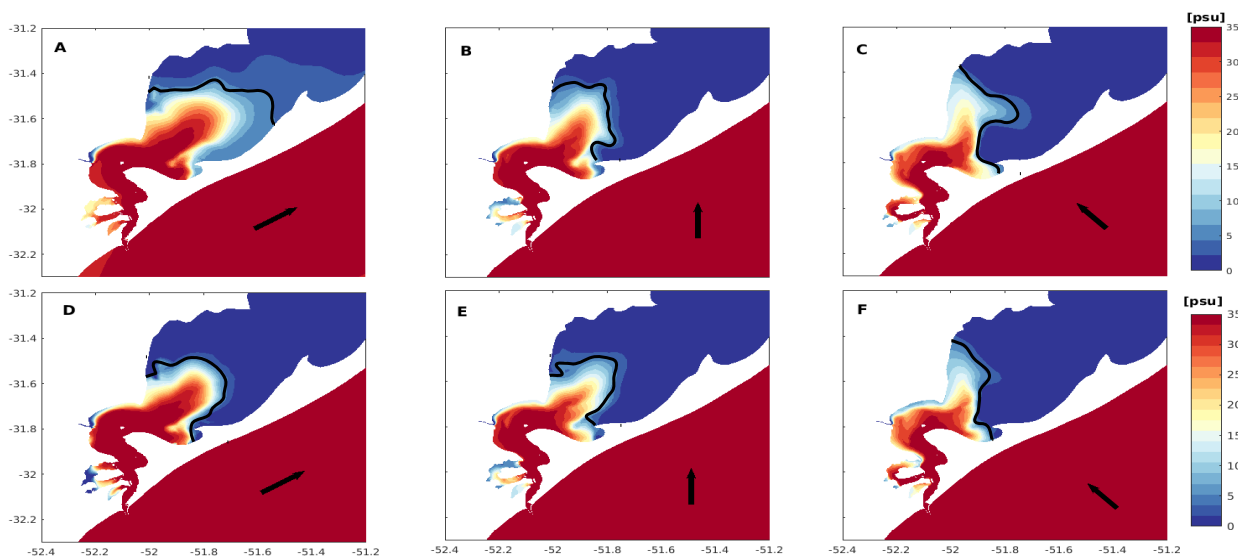


1038 Figure 2: Wind and discharge from 26/12/2002 to 5/01/2003 (left panel) and from 26/12/2011 to
 1039 5/01/2012 (right panel). (A and B) SW wind, (C and D) S wind and (E and F) SE wind. Black dotted
 1040 rectangles represent characteristic periods of Patos Lagoon high discharge (G) during El-Niño (left
 1041 panel) and low discharge (H) during La-Niña (right panel) that were simulated in this study.

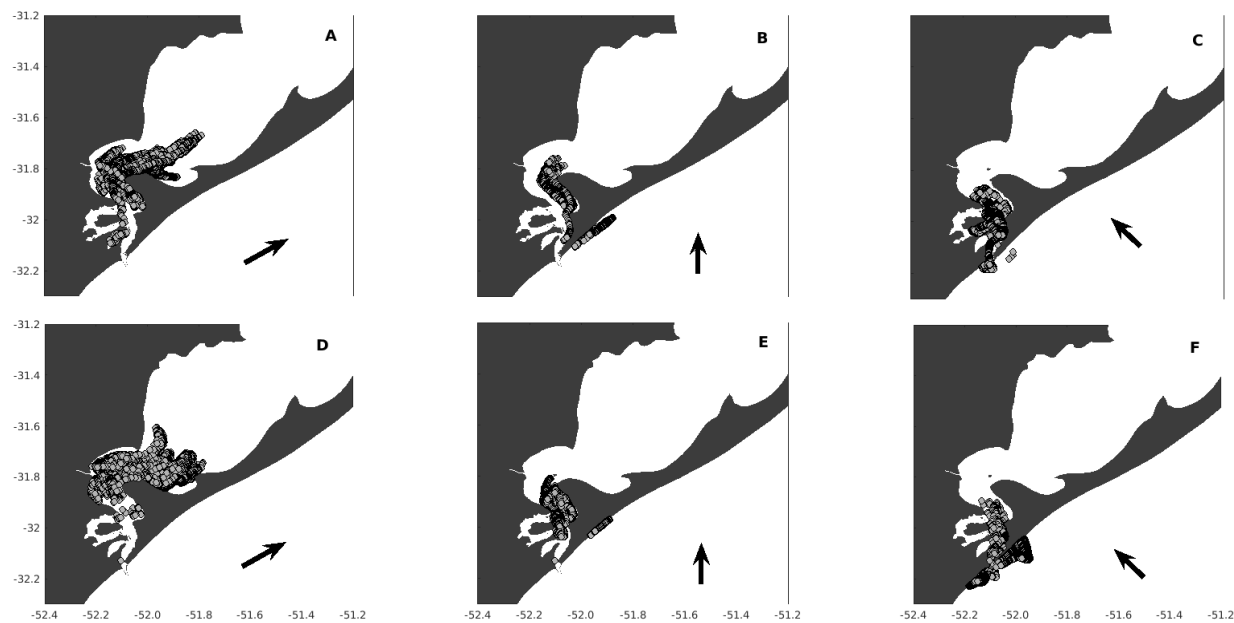




1042 Figure 3: Spatial distribution of salinity excursion at the end of 5 days of simulation during the high
1043 continental discharge condition, considering SW (A and D), S (B and E) and SE (C and F) wind
1044 experiments (black arrows). Results are presented for the old (top panel) and for the new (bottom
1045 panel) jetty configurations. Black line indicates salinity reference of 5 psu.

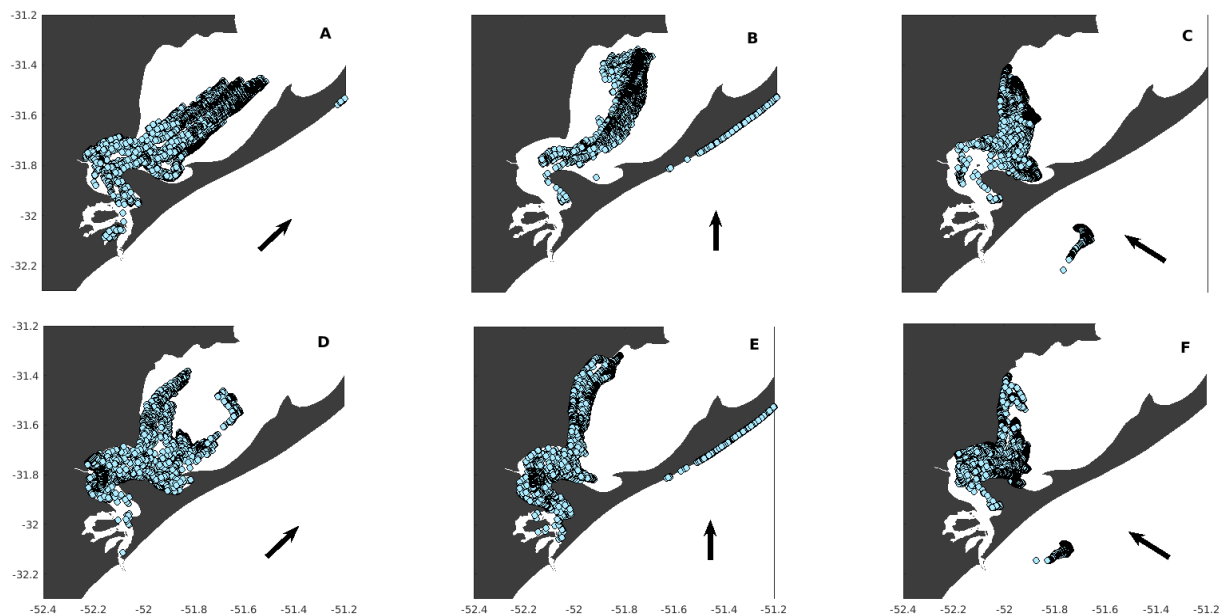


1046 Figure 4: Spatial distribution of salinity excursion at the end of 5 days of simulation during the low
1047 continental discharge condition, considering SW (A and D), S (B and E) and SE (C and F) wind
1048 experiments (black arrows). Results are presented for the old (top panel) and for the new (bottom
1049 panel) jetty configurations. Black line indicates salinity reference of 5 psu.

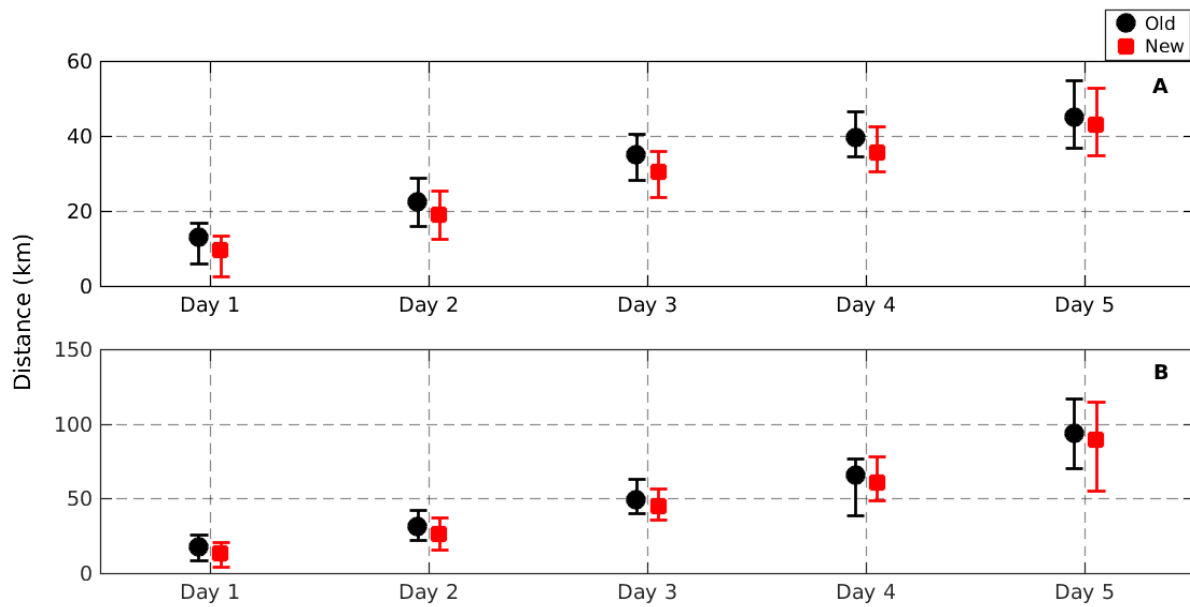




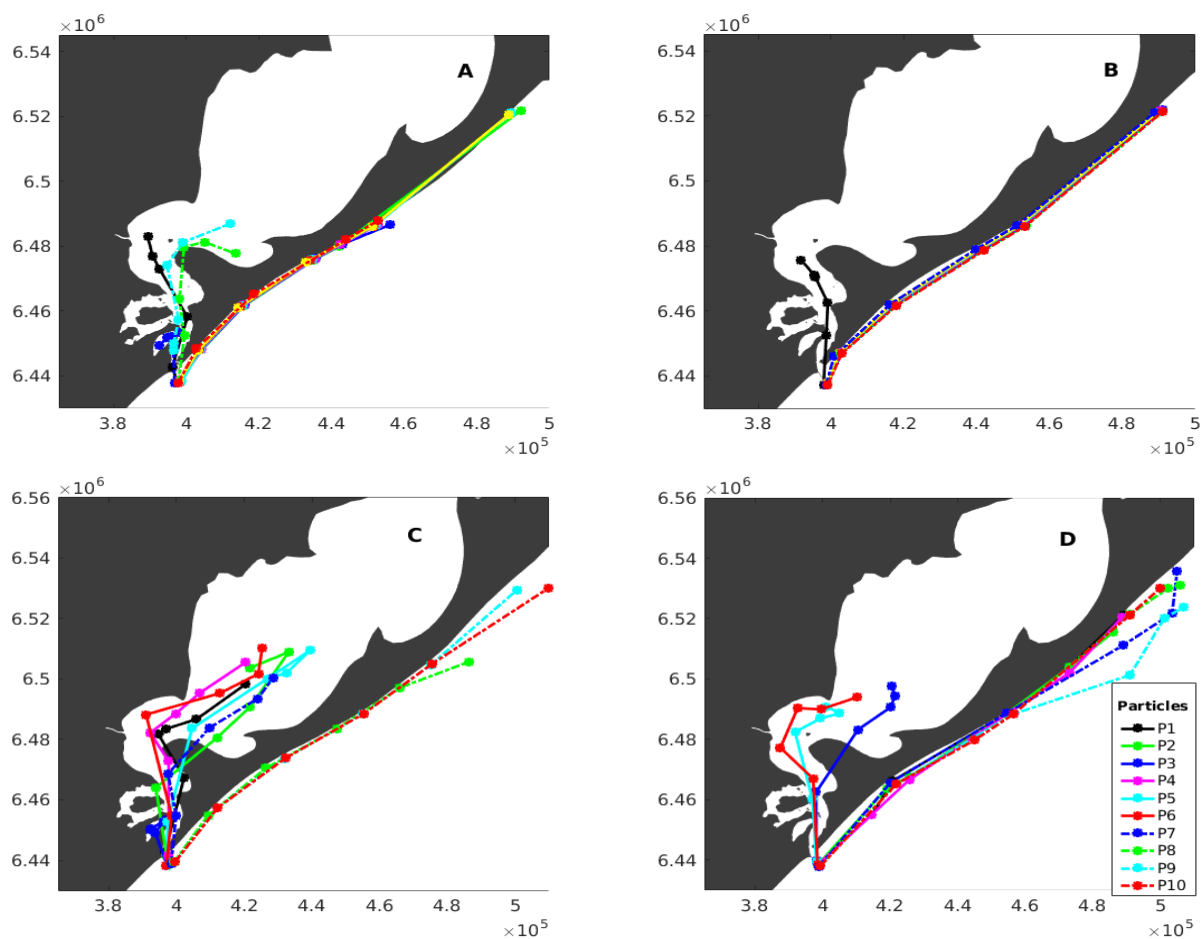
1050 Figure 5: Spatial distribution pattern of excursion of *Micropogonias furnieri* larvae at the end of 5
1051 days of transport, during the period of high continental discharge, considering the SW (A and D), S
1052 (B and E) and SE (C and F) wind experiments. Results are presented for the old (top panel) and for
1053 the new (bottom panel) jetty configurations. Black arrows indicate the wind direction.



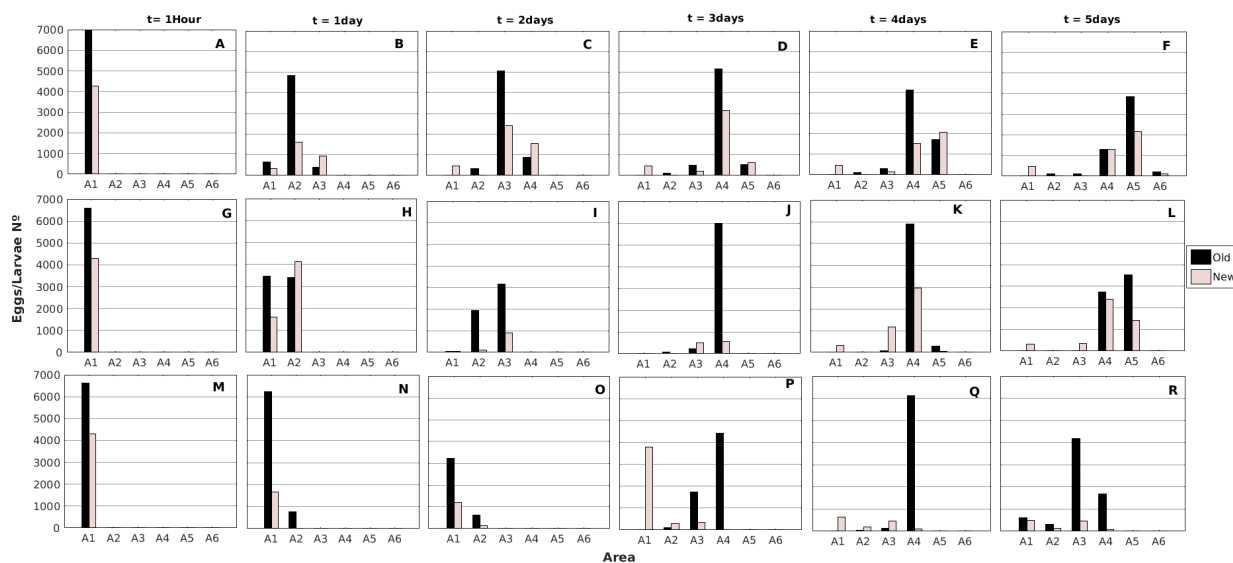
1054 Figure 6: Spatial distribution pattern of excursion of *Micropogonias furnieri* larvae at the end of 5
1055 days of transport, during the period of low continental discharge, considering the SW (A and D), S
1056 (B and E) and SE (C and F) wind experiments. Results are presented for the old (top panel) and for
1057 the new (bottom panel) jetty configurations. Black arrows indicate the wind direction.



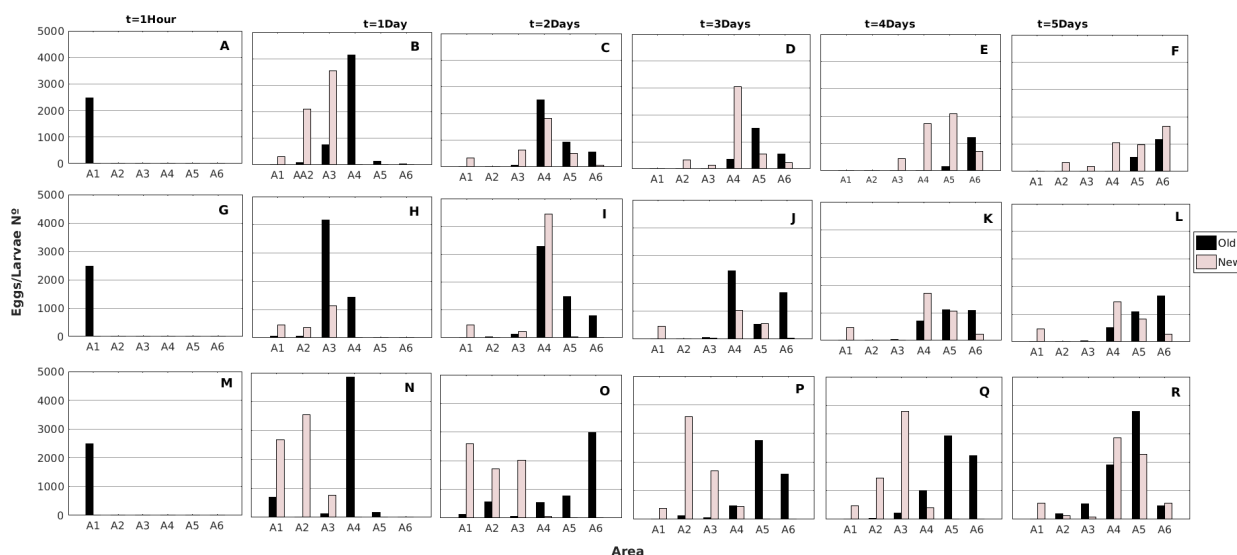
1058 Figure 7: Distribution of the mean distance traveled by *Micropogonias furnieri* larvae sampled
1059 during the SW wind experiment at the end of each of the 5 days (day 1, day 2, day 3, day 4 and day
1060 5), simulated during the period of high water discharge (A) and low water discharge (B), for the old
1061 (black) and the new (red) jetty configuration.



1062 Figure 8: Trajectory of *Micropogonias furnieri* eggs and larvae for the SW wind experiment at the
1063 end of each of the 5 days (1h, day 1, day 2, day 3, day 4 and day 5), during the period of high (top
1064 panel) and low (bottom panel) water discharge for the old (A,C) and new (B, D) jetty configuration.
1065 Particle tracking trajectory during the SW wind experiment, at the end of each of the 5 days of
1066 simulation (1h, 1 day, 2 days, 3 days, 4 days and 5 days, marked dots).



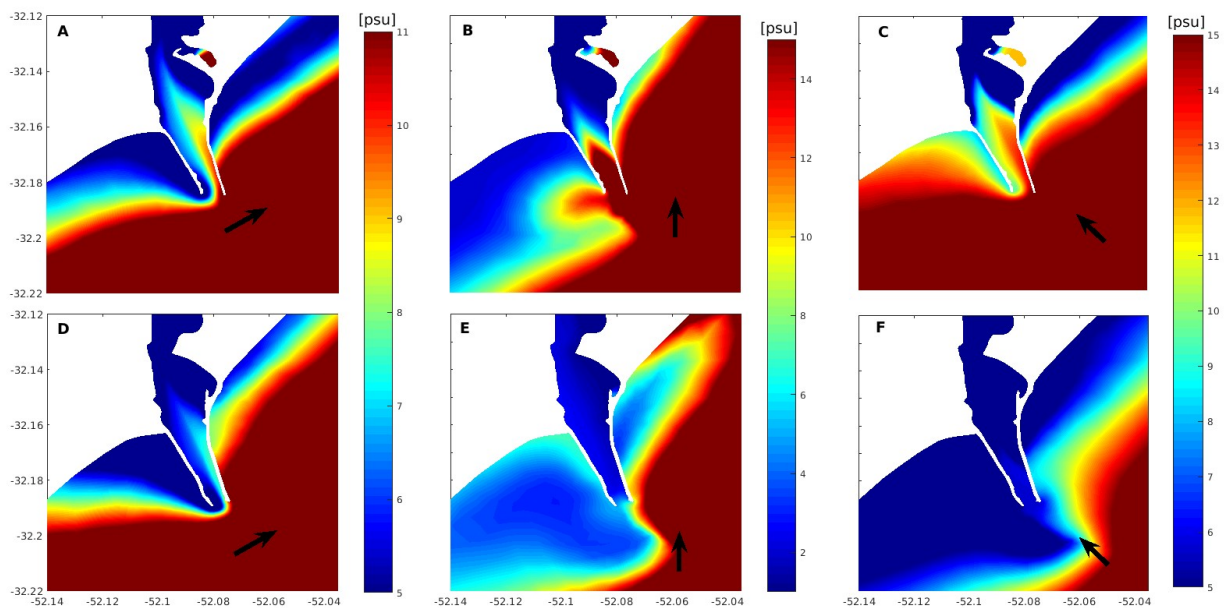
1067 Figure 9: Spatio-temporal distribution of the abundance of eggs and larvae of *Micropogonias*
 1068 *furnieri* in the 5 areas (A1, A2, A3, A4 and A5) at the end of each of the 5 days of simulation (day 1,
 1069 day 2, day 3, day 4 and day 5), for old (blue) and new (yellow) jetty configuration, during the
 1070 period of high continental discharge. Considering the SW (Top panel), S (center panel) and SE
 1071 (bottom panel) wind experiments.



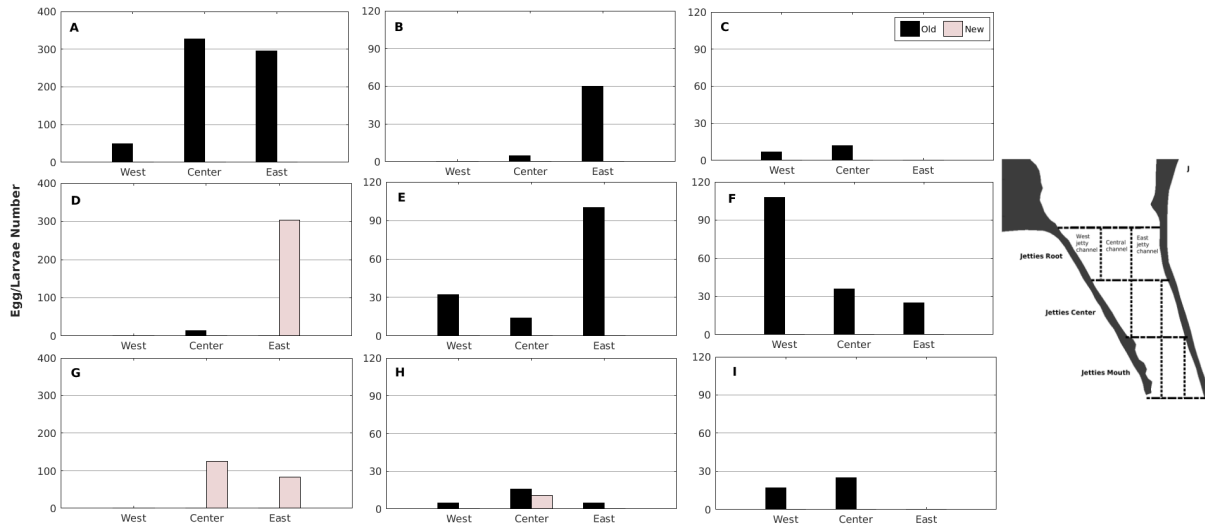
1072 Figure 10: Spatio-temporal distribution the abundance of eggs and larvae of *Micropogonias furnieri*
 1073 in the 5 areas (A1, A2, A3, A4 AND A5) at the end of each of the 5 days of simulation (day 1, day 2,
 1074 day 3, day 4 and day5), for old (black) and new (blue) jetty configuration, during the period of low



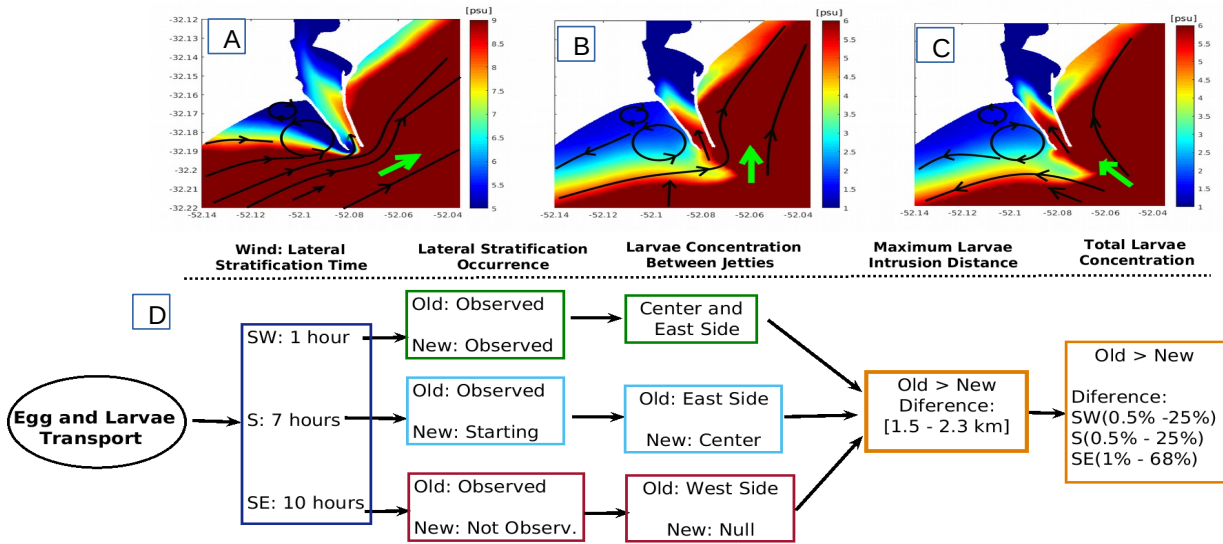
1075 continental discharge. Considering the SW (Top panel), S (center panel) and SE (bottom panel)
1076 wind experiments.



1077 Figure 11: Spatial distribution of salinity in the estuarine mouth during low continental discharge
1078 at: 1h (A and D), 7h (B and E), 10h (C and F), considering the SW (A and D), S (B and E) and SE
1079 (C and F) wind experiments. Results are presented for the old (top panel) and for the new (bottom
1080 panel) jetty configurations. Black arrows indicate the wind direction.



1081 Figure 12: Egg abundance of *Micropogonias furnieri* between the jetties during lateral stratification,
 1082 considering the SW (A, D and G), S (B, E and H) and SE (C, F and I) wind experiments, at: jetties
 1083 root (A, B, C), jetties center (D, E, F), an jetties mouth (G, H, I). During the period of low water
 1084 discharge.



1085 Figure 13: Schematic diagram of the differences in the transport of eggs and larvae of
 1086 *Micropogonias furnieri* from the coastal region to the Patos Lagoon estuary induced by changes in
 1087 the configuration of the jetties.. Coastal circulation induced by SW (A), S (B) e SE (C) winds.
 1088 Black lines and arrows indicate the current velocity. Green arrows indicate the wind direction. (D)
 1089 Diagram of the resulted effects in the eggs and larvae transport.